Studies on the role of RANK/RANKL expression for the skeletal lesions and the effect of anti-RANKL neutralizing antibody in a canine osteosarcoma xenograft model

(イヌ骨肉腫における RANK/RANKL 発現と骨病変との関連ならびに移植マウスモデルにおける抗 RANKL 中和抗体の抗腫瘍効果に関する研究)

上田　綾子

Contents

General Introduction

Canine osteosarcoma (OSA) is one of the most common primary bone tumors with higher prevalence than human OSA. Canine OSA is considered to be an excellent model for understanding pathogenesis, histological appearance and biological behaviors of human OSA (Khanna et al., 2006; Paoloni and Khanna, 2008). Moreover, there have been successful studies provided by using canine models to treat human OSA, such as multimodal chemotherapy followed by limb-sparing (Berg et al., 1992; LaRue et al., 1989; Withrow et al., 1993). Thus, canine OSA is a promising study target to elucidate the molecular pathogenesis and development of novel therapies for both in human and dogs.

Despite a combination of surgery and pre/post-surgical chemotherapy dramatically improved the survival rate in human OSA, such chemotherapy with considerably high doses of drugs cannot be applied for canine patients due to strong toxicity. The 5-year survival rate in human OSA patients is up to 70%, however the survival rate seems to reach to the plateau in the past 20 years (Lamoureux et al., 2008). In dogs, the surgery such as amputation is the most common therapy to alleviate tumor-associated pain and improve quality of life, although the survival rate does not

improve dramatically (Kirpensteijn et al., 1999). There have been some reports using adjuvant chemotherapy (cisplatin and or doxorubicin) subsequent to the surgery (Bacon et al., 2008; Berg et al., 1997; Mauldin et al., 1988; Straw et al., 1991). However, use of adjuvant chemotherapy is not effective to provide dramatic changes in survival rate. Thus, palliative therapy such as surgery, radiation therapy or use of bisphosphonates is prospective to alleviate tumor-associated pain and improve the quality of life (Fan et al., 2009; Fan et al., 2008; Fan et al., 2007; Mayer and Grier, 2006). Therefore, novel efficient therapies to provide both prolongation of survival rate and alleviation of pain are required for both human and canine OSA patients.

In OSA, bone lesions often cause severe pain due to bone destruction and pathological fracture (Boulary et al., 1987). Tumor-induced osteolysis is considered to be associated with osteoclast (OC) activity. OCs are multinucleated cells with 3 to 8 nuclei, derived from monocyte-macrophage lineage precursor cells, and their differentiation is strictly regulated by two essential cytokines, macrophage colony-stimulating factor (M-CSF) and receptor activator of nuclear factor-κB ligand (RANKL) (Tanaka et al., 2005; Yasuda et al., 1998).

RANKL, a member of the tumor necrosis factor (TNF) superfamily, is expressed on the surface of osteoblasts in response to various hormones and cytokines, and binds to its specific receptor RANK expressed on OC precursors. Osteoprotegerin (OPG) is a decoy receptor of RANKL and competitively inhibits the RANK-RANKL interaction. M-CSF regulates the survival and fusion of OC precursors at an early stage (Pixley and Stanley, 2004), while RANKL is essential for the subsequent differentiation and maturation (Lossdorfer et al., 2004).

The binding of RANKL to RANK induces the trimerization of RANK and the recruitment of TNF-associated factor 6 (TRAF6) to the intracellular domain of RANK, which in turn activates downstream signaling pathways such as NF-κB and mitogen-activating protein kinase (MAPK) (Fig.1). This, in turn, leads to the induction of nuclear factor of activated T cells (NFATc1). NFATc1 is a master regulator of OC differentiation and regulates the expression of OC-specific markers such as tartrate-resistant acid phosphatase (TRAP) and calcitonin-receptor (Calcitonin-R) (Boyle et al., 2003; Takayanagi et al., 2002). While attached to the bone surface, OCs generate sealing zones comprising the ringed structure of F-actin (actin ring), which

isolates the resorption area and secretes protons and proteinases such as cathepsin K (Tezuka et al., 1994) and matrix metalloproteinase 9 (MMP9) (Reponen et al., 1994) from highly invaginated cell membranes facing the bone, called the ruffled border.

The RANK/RANKL/OPG are the crucial factors for OCs biology and also known to be involved in the process of bone destruction in both primary and metastatic bone tumors (Wittrant et al., 2004). Tumor cells themselves are unable to resorb bone matrix directly, therefore tumor-mediated OC differentiation is required for bone resorption, which must take place before the tumor cells grow and invade into the bone microenvironment (Wittrant et al., 2004). Bone is rich in growth factors and cytokines, which provide a soil for tumor development and proliferation. Tumor cells are known to express OC-inducing factors such as parathyroid hormone-related protein (PTHrP), interleukin 1 (IL-1), IL-6, IL-8, colony-stimulating factor-1 (CSF-1), and transforming growth factor (TGF)-β1. It is also suggested that several tumor cells produce RANKL, which promotes osteoclastogenesis and induces the growth factor from bone matrix, resulting in tumor proliferation (Akiyama et al., 2008). This vicious cycle is well explained for the primary and metastatic bone tumor development (Fig.2).

The primary bone tumors such as OSA and giant cell tumor are good targets for the OC-targeted therapy, since the involvement of RANK/RANKL in these tumors was reported (Ando et al., 2008; Mori et al., 2009; Mori et al., 2006). Functional RANK expression on murine OSA cells and human OSA patient tissues has been reported by Mori, K. et al. (2007b), where the RANKL-modulated gene expression of RANK-positive OSA cells was also confirmed (Mori et al., 2007).

Although the RANKL-targeted therapies are drawn attention as a novel bone tumor treatment in human, the involvement of these molecules in dogs is unknown. The aim of this study was to clarify the involvement of RANK-RANKL in canine OSA skeletal lesions, to elucidate the function of RANK-expressing OSA cell lines and to clarify the therapeutic effect of anti-RANKL antibody in a xenograft mouse model. In Chapter 1, I first evaluated the expression of RANK and RANKL in *in vitro* and *in vivo* experiments, using the tissues from OSA clinical patients, canine OSA cell lines and tissues from cell line-xenografted mice. In Chapter 2, based on the result from Chapter 1, HMPOS and CHOS cell lines were selected as to determine the function of RANK-expressing OSA cell lines under RANKL stimulation *in vitro*. From the results

of Chapters 1 and 2, the involvement of RANK-RANKL in canine OSA was suggested, therefore I hypothesized that targeting RANKL produced by OSA cell lines may be a prominent therapy in dogs. Thus in Chapter 3, to clarify *in vitro* and *in vivo* function of RANKL produced by OSA cell lines in osteoclastogenesis, low-RANKL expressing cell line (HMPOS) and high-RANKL-expressing cell line (CHOS) was selected. To evaluate the osteoclastogenic potential of canine OSA cells, I first attempted to establish *in vitro* canine OCs differentiation method using M-CSF and RANKL. Using this method, indirect osteoclastogenic capacity of conditioned medium (CM) either from HMPOS or CHOS cell lines was evaluated. Moreover, the anti-resorptive and direct anti-tumoral effect of anti-mouse RANKL-neutralizing monoclonal antibody was elucidated by using CHOS-xenografted mice.

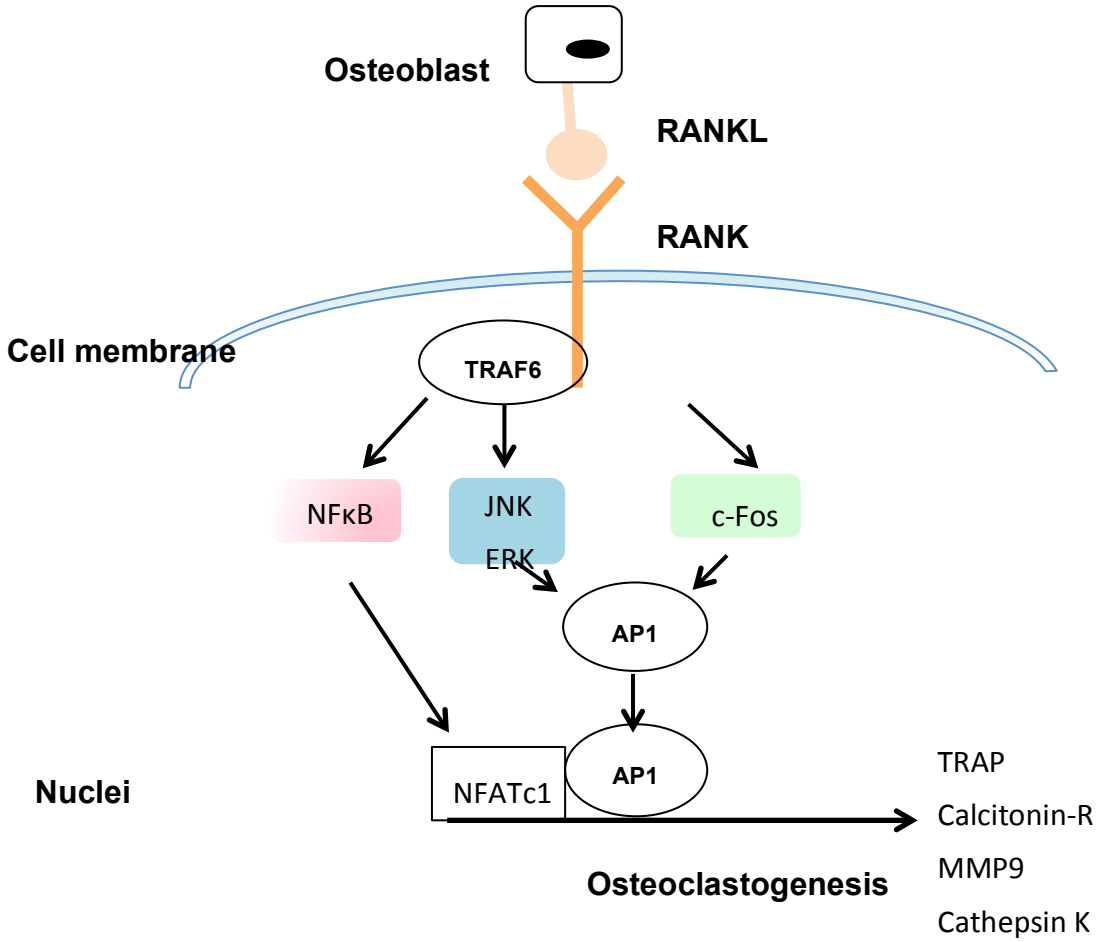

Fig. 1 RANK-RANKL signal transduction pathways in osteoclast

RANKL interacts with the binding site of RANK, resulting in recruitment of TRAF6 to the intracellular domain, and then activates NFκB and MAPK (ERK1/2, JNK) cascades. In addition, expression of c-fos (transcriptional factor which form AP1) is induced. These activated pathways interact with NFATc1 (indispensable factor for OC differentiation) to induce transcription of osteoclastogenic genes.

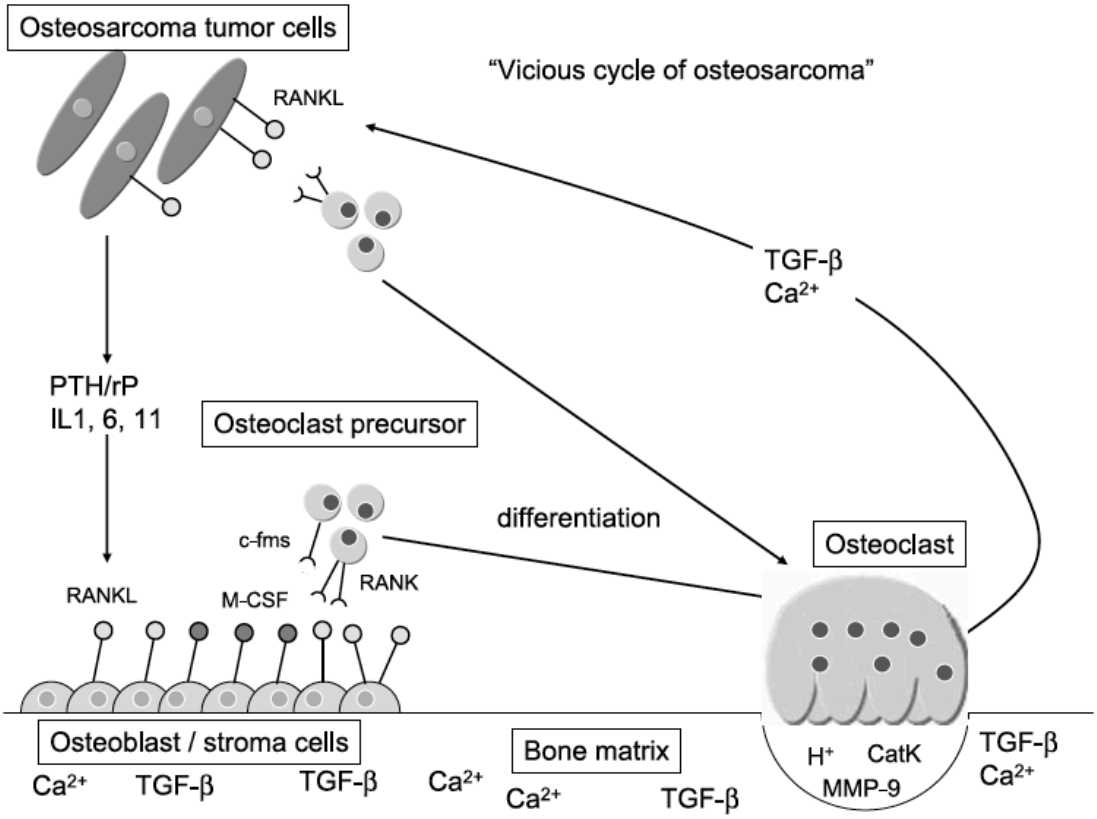

Mol Cancer Ther. 2008 Nov;7(11):3461-9

Fig. 2 The vicious cycle of OSA

In the normal state, RANKL is maily produced in osteoblasts and stromal cells, and binds to OC precursors to induce osteoclastogenesis. This leads to degradation of bone matrix, and since bone is rich in growth factors (eg. TGFβ) and cytokines, resulting in release of these moleculed to promote tumor cell activation and proliferation.

Chapter 1

Expression of RANK/RANKL on the primary tumor tissues of canine OSA patients, canine OSA cell lines, and OSA tissues developed in xenografted mice

Introduction

Canine OSA is commonly seen in middle-aged to older dogs with a range of 7-10 years old, although there are some cases with younger age with shorter survival time (Boston et al., 2006; Spodnick et al., 1992). It is frequently observed in large or giant breeds dogs such as Saint Bernard, Great Dane, Rottweiler, German shepherd, and Golden retriever (McNeill et al., 2007; Norrdin et al., 1989; Ru et al., 1998). Males are slightly more commonly affected than females by 1.5 times, with the exception for the dogs with axial skeleton (excluding rib and spine) and some breeds (Saint Bernard, Great Dane and Rottweiler) (Heyman et al., 1992). Approximately 75% of OSA arises in the appendicular skeleton, and the remaining 24% in axial skeleton and 1% in extraskeletal sites (Liptak et al., 2004; Patnaik, 1990). The front limbs are affected twice as often as the hind limbs, and two common locations are the distal radius and proximal humerus followed by the distal femur, distal and proximal tibia (Knecht and Priester, 1978; Straw et al., 1990).

The accurate diagnosis of bone tumors requires appropriate clinical and radiographic evaluation as well as histology. Dogs with appendicular OSA generally

show lameness due to tumor-associated pain and swelling at the primary site. Radiographic appearance varies from osteolysis to osteogenic changes such as "sun-burst" appearance, which may cause the fragile bones and sometimes pathological fracture. Histological diagnosis is made based on the World Health Organization Collaborating Centre for Comparative Oncology (WHO). OSA is defined as "*a primary malignant tumor of mesenchymal tissue that gives rise to a variety of patterns, but always includes the production of bone by malignant osteoblasts*". There are variety of cell types involved in OSA, and the current histological classification is as follows; poorly differentiated, osteoblastic, chondroblastic, fibroblastic, telangiectatic and giant cell types (Slayter et al., 1994, (Loukopoulos and Robinson, 2007).

The outcome of canine OSA is poor in the consequence of high metastatic potential to the lung at an earlier stage. Lung metastasis is frequently found at the diagnosis of the primary site (Ling et al., 1974). Various prognostic factors have been reported, including age under 5 years old related to shorter survival time (Loukopoulos and Robinson, 2007) and an increase in tumor size is related to more lung metastasis and invasion to adjacent soft tissues (Forrest et al., 1992; Misdorp and Hart, 1979).

Higher histological grade (Kirpensteijn et al., 2002), higher mitotic index (Kirpensteijn et al., 2002; Loukopoulos and Robinson, 2007), higher total serum alkaline phosphatase (TALP); >110 U/L (Ehrhart et al., 1998; Garzotto et al., 2000; Selvarajah et al., 2009) and metastatic spread to the lung (Boston et al., 2006) or regional lymph nodes (Hillers et al., 2005) are also the indices of prognosis. Moreover, tumor location is also related to prognosis; OSA at the humerus has shorter survival time (Bergman et al., 1996), while these at the mandible has favorable outcome (Dickerson et al., 2001). Histological subtypes are also reported and OSA of fibroblastic subtype is reported to have more favorable prognosis (Loukopoulos and Robinson, 2007; Misdorp and Hart, 1979).

In human OSA or metastatic bone tumors, bone lesions commonly cause severe pain due to osteolysis and osteogenesis (Bryden et al., 2002; Mundy, 2002; Nelson et al., 1995). Osteolysis has been reported to relate to OC activity and OC regulating factors, such as RANK/RANKL/OPG axis. Increased OC activity at the primary site was positively correlated with tumor aggressiveness (Avnet et al., 2008), and RANKL on the primary tissue was also correlated to less response to preoperative chemotherapy and poor event-free survival in human OSA patients (Lee et al., 2010).

Possible involvement of RANKL in canine OSA pathophysiology was also reported, and variety of canine and feline bone tumor tissues, including OSA, showed higher RANKL expression. However, this higher RANKL expression was not correlated with clinical variables including radiographic characterization and bone mineral density (BMD) (Barger et al., 2007).

Based on these findings in human and canine OSA, the RANK-RANKL might be a novel therapeutic target for OSA. The aim of this Chapter was to investigate the expression of RANK and RANKL on tissues from canine OSA patients by using immunohistochemical analysis and to evaluate correlation between their expressions and clinical variables. In addition, their expression on 4 canine OSA cell lines established in our laboratory was determined, then the significance of these expressions on skeletal changes was analyzed using a xenograft mouse model using these cell lines.

Section 1: Expressions of RANK and RANKL on primary tissues from canine OSA patients and OSA cell lines

Materials and Methods

Patients

A total of 26 OSA samples were obtained from dog patients that were referred to Veterinary Medical Centre at the University of Tokyo, between 2006 and 2011. The clinical information including age, gender, breed (large breed; ≥20kg, medium breed 10-20kg, small breed; ＜10kg), primary site, serum ALP levels, histological subtype, lung metastasis and survival time was collected from the medical records and telephone interviews to either clients or referred veterinarians. Serum ALP was measured by using DRI-CHEM 7000V (FUJIFILM, Tokyo, Japan) and over 110 (≥ 110 U/l) was considered as high, while below 110 (<110) was considered as normal (Ehrhart et al., 1998). Histological subtype was evaluated by diplomates of Japanese College of Veterinary Pathologist of the Laboratory of Veterinary Pathology, the University of Tokyo, according to WHO classification. Lung metastasis was confirmed

on thoracic radiography. Survival time was defined as the time from the day of diagnosis to death.

Cell culture

Canine OSA cell lines, POS, HMPOS (cloned cell line of POS), OOS and CHOS established from spontaneous patients in our laboratory, were used in this study (Barroga et al., 1999; Hong et al., 1998; Kadosawa et al., 1994). Cells were cultured in RPMI-1640 medium (Wako Pure Chemical Industries, Osaka, Japan) supplemented with 10% fetal bovine serum (FBS) (Gibco BRL, Grand Island, NY, USA) and 5mg/l gentamicin sulfate (Sigma Chemical Co., St. Louis, MO, USA) at 37ºC in a humidified atmosphere of 5% CO_2.

Antibodies

The primary antibodies used were as follows: rabbit anti-RANK polyclonal antibody (Santa Cruz Biothecnology, Santa Cruz, CA, USA); rabbit anti-RANKL antibody (ALEXIS, Lausen, Switzerland) and mouse anti-actin antibody (Millipore,

Tenecula, CA, USA). The dilutions of these antibodies used for immunohistochemistry (IHC), immunocytochemistry (ICC) and Western blot analysis (WB) were shown in the following table.

Antibody	Dilutions		
	IHC	ICC	WBC
RANK	1:50	1:50	1:200
RANKL	1:50	1:50	1:200
Actin			1:10,000

Histopathology and Immunohistochemistry (IHC)

All specimens were fixed with 10% neutralized buffered formalin, decalcified with 10% EDTA and then paraffin-embedded using a standard protocol. The tissues were sectioned into 4 μm in thickness and stained with hematoxyline and eosin (HE), and examined with a light microscope (Olympus BX51, Tokyo, Japan).

Tartrate-resistant acid phosphatase (TRAP) staining was also performed to detect activated OCs according to the method previously reported (Kondo et al., 2006). Briefly, the sections were stained with TRAP solution (N-Ndimethylformamide, Naphtol AS-Mx phosphate, TRAP buffer, Fast Red Violet LB salt) at 37ºC for 30 minutes. Then they were counterstained with 0.1% brilliant-green for 5 minutes.

IHC was performed on the sections using a DAKO-ENVISION(＋) kit/HRP (DAB) (DAKO Diagnostics Japan Inc, Kyoto, Japan). The endogenous peroxidase activity was minimized using 3% H_2O_2 for 10 minutes and non-specific antibody reaction was inhibited by incubating with 5% normal goat serum (Sigma) at room temperature for 1 hour. The primary antibodies were reacted for over night at 4ºC. Cross reactivity of the antibodies against canine was determined previously (Barger et al., 2007; Spahni et al., 2009). After washing with PBS-T for 3 times, sections were treated with the HRP-conjugated antibody against rabbit immunoglobulin at room temperature for 30 minutes. Then sections were visualized with a liquid 3,3'-diaminobenzidine (DAB)/hydrogen peroxidase solution, and counterstained with Mayer's hematoxylin. Negative controls were incubated with a negative control reagent (universal negative control for N-series rabbit primary antibodies).

Scoring system of RANK and RANKL expression and TRAP staining on the tissues of OSA patients

The immunohistochemical staining for tissue sections were analyzed by a light microscope (Olympus) at x 200 magnification. The percentage of positive cell staining area over the mean ratio of random 5 fields was calculated by Image J (NIH, Bethesda, MA, USA). The immunoreactivity was interpreted by semi-quantitative scoring system described by Kim et al. (2007). The proportional scoring system was used as follows; 0=no positivity; 1= positive in <1/3 of tumor cells; 2=positive in 1/3-2/3 of tumor cells; and 3=positive in >2/3 of tumor cells. Intensity scores were defined as follows; 0= no staining; 1=moderate staining; and 2=strong staining. The overall scores were calculated by summing intensity scores and proportional scores. Additionally, overall scores of 0-3 were defined as low expression, and scores 4-5 were defined as high expression (Kim et al., 2007).

TRAP-positive cells with more than 3 nuclei were counted as OCs (Nannuru et al., 2009) and the number of OCs were calculated as lower (<4) or higher (≥4) than 4 OCs as the mean ratio of random 5 fields at a magnification of x200.

Immunocytochemistry (ICC)

OSA cell lines at a density of $5x10^3$ cells/well were seeded onto Lab Ⅱ 8-well chamber slides (Thermo Fisher Scientific Inc., Waltham, MA, USA) coated with poly-L-lysine and incubated at 37℃ for 24 hours. After aspirating culture media, cells were fixed with 4% paraformaldehyde / PBS at room temperature for 30 minutes with gentle shaking. Then, they were proceeded by the same procedure as immunohistochemistry analysis described in IHC.

Western blot analysis (WB)

Protein expression of RANK and RANKL on OSA cell lines was evaluated by WB. Protein lysates were made from each cell line after 24 hours of serum starvation. Cells at 70-80% confluence were washed 3 times with cool PBS and lysed in RIPA buffer (50 nM Tris-HCl, 150 nM NaCl, 0.1% 5 M EDTA, 1% Triton-X, 0.1% SDS, 1 complete Mini tablet/10 ml H_2O) (Roche Diagnostics, Indianapolis, IN, USA). Protein concentrations were measured by BCA protein assay reagent (Thermo Fisher Scientific Inc.). Lysates were mixed with 4x sample buffer and 30 μg of each protein lysates were

subjected to SDS-PAGE gel containing 12% of acrylamide. Once the proteins were separated, they were blotted onto a polyvinylidene (PVDF) membrane (Bio-rad, Hercules, CA, USA). The membranes were blocked with 5% of skin-milk in TBS-T at room temperature for 1 hour. Then they were incubated with the primary antibodies at 4 ºC overnight with vigorous shaking. The membranes were washed with TBS-T and incubated with horseradish peroxidase (HRP)-conjugated antibody against mouse IgG or rabbit IgG (GE Healthcare UK Ltd., Buckinghamshire, England) at room temperature for 1 hour. The antibody-antigen complex was visualized by the enhanced chemiluminescence (ECL) detection system (GE Healthcare UK Ltd.).

Statistical analysis

Correlations between clinicopathological variables and expressions of RANK, RANKL and TRAP were analyzed by the Chi-square test. Kaplan-Meier method and log-rank test were performed to compare survival time between OSA patients with high and low expression of RANK, RANKL and TRAP. $P<0.05$ was considered as statistically significant.

Results

Clinicopathological variables in canine OSA patients

Table.1.1.1 shows the clinicopathological variables in 26 patients diagnosed as OSA. Twenty-four (92.3%) patients were over 5 year old and the median age at the time of diagnosis was 9.8±2.9 years old (range 1.9-14.4 years). Females (61.5%) were more common than males (38.5%) in the present study. The breeds of the patients varied from large breeds (16 cases), medium breeds (7 cases), and small breeds (3 cases). The most common breed enrolled in this study was Golden Retriever (26.9%). Hind limbs were more affected (5 femur and 6 tibia) among the sites affected. Serum ALP levels were high in 23 cases (88.5%) and normal in the remaining 3 cases (11.5%) with the median value of 678 IU/l (range 68-6411). Histological subtypes were classified as follows; 17 osteoblastic (65.4%), 5 fibroblastic (19.2%), chondroblastic (7.7%) and giant cell type (7.7%). Typical findings of these subtypes are shown in Fig.1.1.1. Lung metastasis was observed only in 6 cases (23.1%), and remaining 23 cases (76.9%) did not show lung metastasis at the diagnosis. The median survival time

was 291 days (range 5-1139 day) after the diagnosis and 4 cases (15.4%) were still alive.

TRAP staining in the tissues of OSA patients

Fig.1.1.2 shows the typical findings of TRAP-positive cells on the tissues of OSA patients with OC numbers being calculated as <4 or ≥ 4. TRAP-positive cells with <4 were observed in 23 of 26 patients (88.4%) and remaining 3 (11.6%) exhibited ≥ 4 OCs, and there were no correlations between clinical variables and OC number.

Expression of RANK/RANKL on the tissues of OSA patients

Fig.1.1.3 demonstrates the representative expression pattern of both high and low expression of RANK (A) and RANKL (B) on the tissues from OSA patients.

Table 1.1.2 shows correlations between RANK/RANKL expression and clinicopathological variables. Twenty-three of 26 OSA patients (88.4%) showed positive RANK expression, among which 20 showed high score (≥4) and 3 (11.5%) showed low score (<4). Remaining 3 (11.5%) showed negative. Twenty-two of 26 OSA

patients (84.6%) showed RANKL expression, among which 13 (50%) showed high score (≥4) and 9 (34.6%) showed low score (<4). Remaining 4 (15.3%) was negative. RANK expression was significantly correlated with age (p=0.007), however correlations with the other clinical variables were not found. RANKL expression was not correlated to any of clinical variables, while there was a significant correlation between RANKL expression and number of OCs (p=0.04).

Correlation of RANK, RANKL expression and number of OCs with survival of OSA patients

Fig.1.1.4 shows survival curve obtained by Kaplan-Meier method. There were no significant differences in survival time according to the expression levels of RANK and RANKL. Furthermore, no statistical correlation was observed between the number of OCs and survival time.

Expressions of RANK and RANKL on canine OSA cell lines

The morphology of canine OSA cell lines enrolled in this study is shown Fig.1.1.5. Morphology of each cell line was as follows: HMPOS; polygonal cell, POS; mixed with spherical, fibroblastic and polygonal cells, OOS; mixed with spherical, fibroblastic, polygonal cells and giant cells, and CHOS; fibroblastic cells. Fig.1.1.6 shows immunocytochemical findings of these 4 cell lines. The expression of RANK and RANKL was observed on the membrane and cytoplasm of all OSA cell lines. Fig.1.1.7 shows WB analysis for RANK and RANKL of 4 OSA cell lines. RANK protein was expressed in all cell lines. The highest expression was observed in POS, followed by OOS, HMPOS and CHOS in order. RANKL protein was expressed in all cell lines and the highest expression was observed in CHOS, followed by OOS, POS and HMPOS in order.

Discussion

In this study, 26 patients were enrolled, among which 24 were over 5 years old with the median age of 9.8±2.9 years, similar to the previous reports (Boston et al., 2006; Spodnick et al., 1992). Controversial to the literature (Heyman et al., 1992; Knecht and Priester, 1978; Straw et al., 1990), females were more common than males and hind limbs were frequently affected in this study. Golden retriever was the most common breed, although a variety of breeds were included (McNeill et al., 2007; Norrdin et al., 1989). The predominant histological subtype was osteoblastic with relatively higher serum ALP, similar to the previous reports (Ehrhart et al., 1998; Hammer et al., 1995).

TRAP-positive cells on the tissues of 23 out of 26 OSA patients (88.4%) showed <4, and remaining 3 (11.5%) showed ≥ 4. Avnet et al. reported that 10 in 16 human OSA patients showed positive OCs in tissues, and measurement of serum TRAP by ELISA assay confirmed that increased OC activity positively correlated to the presence of lung metastasis (Avnet et al., 2008). However, I found that canine OSA

patients enrolled in this study showed no correlations between clinical variables including lung metastasis and number of OCs. The difference between the two reports by Avent et al. and this study may be due to the conditions of tissues enrolled in each study. Tissues in their study were obtained by biopsy or total resection, thus the distribution of OCs might be imbalance.

The correlations between RANK/RANKL expression and clinicopahologic variables were also evaluated. High-RANKL-expressing tissues from the primary OSA patients tended to be fibroblastic subtype with osteolysis based on survey radiography. Although 88.4% and 84.6% of patients showed RANK and RANKL expression, respectively, and there were significant correlations between RANK expression on tumor tissues and age of patients, and between RANKL expression and number of OCs on tumor tissues. However, there was no other significant correlation to clinical variables, similar to the previous report (Barger et al., 2007). These results may be similar in the study by Mori et al. (2007) using human OSA tissues. They found RANK expression on 11 of 19 tissues of human clinical OSA patients, in which worse response to the standard chemotherapy was observed. Furthermore, similar to the report in Barger

et al. there was no apparent correlation with its expression to age, sex, histological type and tumor localization (Mori et al., 2007). Meanwhile, high RANK-expressing patients tended to have shorter survival, while there was no statistical correlation. Relatively small number of canine patient in this study may be a weak point as in the report by Mori et al. Additional limitation of this study was that most of the tissues obtained by patients were only one section from the primary lesion, thus further analysis using an increased number of patients and multiple sections from each patients should be performed.

Four canine OSA cell lines showed both RANK and RANKL expression at the protein level. Based on the WB analysis, HMPOS cells showed relatively higher RANK protein expression, while CHOS cells showed the lowest expression. On the contrary, CHOS cells showed the highest protein expression of RANKL, while HMPOS cells showed the lowest expression.

HMPOS was the most malignant cell line among the 4 cell lines used in this study. Morphology of HMPOS cells was osteoblastic and the proliferation was fast (Kadosawa et al., 1994), while that of CHOS cells was fibroblastic and the growth rate

was slow. Further study is required to clarify the involvement of RANK and RANKL on pathogenesis of canine OSA using a xenograft mouse model.

Section 2: Expressions of RANK and RANKL on tissues developed in a xenograft mouse model

Materials and Methods

Xenograft mouse model

Five-week-old BALB/c, nu/nu male mice (Japan SLC, Inc., Tokyo, Japan) were used (n=5 per group) in this study. They were housed under the pathogen free condition, and fed with sterile food and water *ad libitum.* This experiment was conducted according to the Guideline approved by the Animal Care Committee of the Graduate School of Agricultural and Life Sciences, the University of Tokyo.

Animals were kept in the cage for a week before experimental procedures. Three days before transplantation, all mice were irradiated with a dose of 4 Gy by an orthovoltage irradiation unit (Hitachi Medical Corporation, Tokyo, Japan). Under anesthesia with diethylether, each cell line ($1x10^5$ cells/10 μl) in 50% Matrigel (BD, Bedford, MA, USA) was injected into the right proximal tibia using a 25 G needle with

"drill-like" movement according to the method reported by Berlin et al (1993). Once the bone cortex was transversed, cell suspensions or vehicle (medium) were injected using an allergy syringe (BD) and placed the needle for 10 seconds to settle the cells. Mice were sacrificed at 1^{st}, 3^{rd} and 5^{th} week after the transplantation.

Tumor volume

The tumor volume was measured every three days after transplantation. The volume was calculated by the following formula; volume (mm^3)=$4/3[1/4(L+S)]^2$, where L and S are the largest and smallest perpendicular tibia diameters, respectively (Berlin et al., 1993).

Histopathology

Bone lesions of the tibia were fixed with 10% buffered formalin for 5 hours, followed by acid decalcification in 10% EDTA solution at 4 ºC for 2 to 3 weeks. The lung was also fixed with 10% buffered formalin for 2 days. The tibia and lung were

then paraffin-embedded, sectioned longitudinally at 3 μm and 2 μm in thickness, respectively, and stained with HE and TRAP staining.

Immunohistochemistry

IHC for RANK and RANKL expression on tissue sections was performed as described in Chapter 1-1.

Micro-computed tomography (μ-CT)

Both the transplanted and the contralateral tibia of each animal were mounted in the CT specimen tube and placed securely into a desktop X-ray μ-CT system (SMX-90CT, Shimadzu, Kyoto, Japan). Images were obtained at 50 kV (X-ray tube voltage) and 110 μA (tube electric current). Three-dimensional image analysis program (TRI/3D-BON, Ratoc System Engineering, Tokyo, Japan) was used to reconstruct three-dimensional images. The bone samples were stored in 70% ethanol at room temperature before the analysis.

Statistical analysis

The mean and standard deviation (SD) values of the primary tumor volume and the number of lung metastatic nodules were calculated. The changes were compared by using Student's *t*-test and $p<0.05$ was considered statistically significant.

Results

Tumor volume in the xenografted mice

Fig.1.2.1 (A) and (B) show the gross appearance of tumor mass developed in the tibia of HMPOS- and CHOS-xenografted mice, and (C) shows the change in tumor volume at the primary site of the xenografted mice. Tumor growth at the tibia in HMPOS-xenografted mice was significantly faster and larger than that in CHOS-xenografted mice ($p<0.05$).

Histopathological findings of tissues from the xenografted mice

Fig.1.2.2 shows histopathological findings of the primary lesions and metastatic nodules obtained from HMPOS- and CHOS-xenografted mice. Fig.1.2.2 (A) shows tissues developed in HMPOS-xenografted mice with typical histopathological findings of osteoblastic OSA with much osteoids. TRAP staining showed that OCs were not evident at the interface between the tumor and bone. Tissues developed in CHOS-xenografted mice showed typical findings of fibroblastic OSA and OCs were

clearly observed at the interface between the tumor and bone cortex. Fig.1.2.2 (B) confirmed that multinucleated cells were all TRAP-positive OCs. Metastatic nodules were observed only in a HMPOS-xenografted mouse and the number of the nodules showed a significant increase at the end of the observation period, while lung metastasis was not observed in CHOS-xenografted mice (Fig.1.2.2. C, Table.1.2.1).

IHC was performed on the primary lesions developed in HMPOS- and CHOS-xenografted mice (Fig.1.2.3). On the tissue in HMPOS-xenografted mice, RANK was clearly expressed positive, while RANKL was not expressed. The similar findings were also obtained in the metastatic lung lesions in these mice (Fig.1.2.3 C). On the primary tissues developed in CHOS-xenografted mice, showed expression of both RANK and RANKL.

μ-CT findings

Fig.1.2.4 shows μ-CT findings of the tibia. HMPOS-xenografted mice showed destruction of the tibial cortex and invasion to the bone marrow at the 3rd week. At the 5th week, tumor growth was aggressive and destroyed epiphyseal region and

extended to the outside of the tibia (Fig.1.2.4 A). CHOS-xenografted mice showed osteolysis at the 3rd week and the lesion became larger at the 5th week. The lesion seemed to show osteolysis of the bone cortex without invasion into the surrounding tissues (Fig.1.2.4 B).

Discussion

Significant differences in the rate of tumor development were observed between HMPOS- and,CHOS-xenografted mice. Radiographic and histopathological findings at the transplantation site were completely different between the two.

HMPOS-xenografted mice started to develop a larger tumor mass at the 3rd week, while CHOS-xenografted mice did not show apparent change in tumor volume at this stage. The method used for the measurement of primary tumor volume was indirect. Since the size was calculated by measuring the largest and smallest perpendicular tibia diameters including soft tissues, thus the size change due to tumor growth could only be seen when the tumor invaded into the surrounding tissues such as HMPOS-xenografted mice. Furthermore, lung metastatic nodules were found only in HMPOS-xenografted mice, suggesting the malignancy of HMPOS cell line.

Based on histopathology, tissues from HMPOS-xenografted mice did not show clear OCs at the interface of the tumor and bone tissues, while CHOS-xenografted mice showed the increase in the number of OCs at the interface. On IHC, RANK

expression was observed on primary tissues of both xenografted mice, however RANKL expression was only observed on CHOS-xenografted mice. Metastatic nodules seen in the lung of HMPOS-xenografted mice showed similar expression pattern as the primary lesion with positive in RANK expression and negative in RANKL.

There have been accumulating evidences, which support the correlation between loss of OCs and formation of lung metastasis. Endo-Munoz et al. (2010) reported that primary tissues of malignant OSA patients with lung metastasis revealed lower expression of an OC-specific marker, ACP5/TRAP, than those without lung metastasis. Additionally, OC inhibition by zoledronate increased the metastatic nodules in xenograft mouse models, while the fulvestrant (estrogen antagonist which blocks the estrogen receptor) treatment increased the number and activity of OCs, leading to less lung metastasis. Moreover, the study on the effect of OCs loss on metastatic OSA cell lines *in vitro* revealed that the migration of tumor cells was inhibited by presence of OCs conditioned medium (CM), while that CM from bone marrow cells increased the migration by 5-fold (Endo-Munoz et al., 2010). Based on these results, they concluded that the loss of OCs at the primary lesion contributed to the metastatic potential of OSA

although its mechanism was still not clear (Endo-Munoz et al., 2010). These reports support the relations in this experiment that low-RANKL-expressing HMPOS cell line may be related to the malignancy of its behavior in nude mice with aggressive tumor growth and loss of OCs at the interface of the tumor and bone tissues.

The three-dimensional images obtained on μ-CT also showed dramatic skeletal differences between HMPOS- and CHOS-xenografted mice. HMPOS-xenografted mice showed osteogenic and aggressive invasion to the surrounding soft tissues, leading to the much larger size. However, CHOS-xenografted mice showed osteolysis at the primary site, while no apparent invasion to the surrounding soft tissue was observed. These findings were resulted from RANKL protein expression on OSA cell lines. RANKL expression was lowest in HMPOS and highest in CHOS among cell lines. Since RANKL may be a crucial OCs inducing factor, tumor-induced osteolysis seen in CHOS-xenografted mice may be related to RANKL production by CHOS cell line, promoting osteoclastogenesis *in vivo*.

This study confirmed that OC was involved in tumor-induced osteolysis in the xenograft mouse model. It may be suggested that RANKL production by canine OSA

cells promotes osteoclastogenesis and releases the growth factor from the bone matrix. To elucidate the involvement of RANK-RANKL on the pathophysiology of canine OSA, further studies on function of RANK-expressing OSA cell line under RANKL stimulation should be identified.

Clinicopathological Variables	Value
No. of patients	26
Age at diagnosis	Median 9.8±2.9 years old (1.4–14.4)
<5	2 (7.7%)
≥5	24 (92.3%)
Gender	
Male	10 (38.5%)
Female	16 (61.5%)
Breed	
Golden Retriever	7 (26.9%)
Labrador Retriever	3 (11.5%)
Border Collie	2 (7.6%)
Akita	2 (7.6%)
Boxer	1 (3.8%)
Great Pyrenees	1 (3.8%)
Mix	6 (23.0%)
Others	4 (15.4%)
Primary site	
Humerus	3 (11.5%)
Radius	1 (3.8%)
Femur	5 (19.2%)
Tibia	6 (23.1%)
Maxilla	1 (3.8%)
Mandible	3 (11.5%)
Vertebrae	1 (3.8%)
Rib	2 (7.7%)
Others	4 (15.4%)
ALP (IU/l)	Median 678 (68–6411)
Normal	3 (11.5%)
High	23 (88.5%)
Histological subtype	
Osteoblastic	17 (65.4%)
Fibroblastic	5 (19.2%)
Chondroblastic	2 (7.7%)
Giant cell	2 (7.7%)
Lung metastasis	
Negative	20(76.9%)
Positive	6 (23.1%)
Survival time (day)	Median 291 (5–1139)
death	22 (84.6%)
alive	4 (15.4%)

Table.1.1.1 Clinicopathological variables in 26 canine OSA patients

	RANK				RANKL			
	Total	High	Low (−)	p−value	Total	High	Low (−)	p−value
No. of patients	26	20	3 (3)		26	13	9(4)	
Age								
<5	2	0	1 (1)	0.007*	2	1	0(1)	0.91
≥5	24	19	3 (2)		24	12	9 (3)	
Gender								
Male	10	7	2 (1)	0.37	10	6	2 (2)	0.9
Female	16	12	2 (2)		16	7	7 (2)	
Primary site								
Appendicular	16	12	4	0.41	16	8	8	0.69
Others	10	8	2		10	4	6	
Serum ALP								
Normal	3	3	0	0.31	3	2	1	0.45
High	23	17	6		23	10	13	
Histological subtype								
Osteoblastic	17	13	1 (3)	0.57	17	8	6 (3)	0.9
Fibroblastic	5	3	2		5	3	1 (1)	
Others	4	4	0		4	2	0	
Lung metastasis								
Negative	20	16	4	0.1	20	9	11	0.32
Positive	6	4	2		6	3	3	
Osteoclasts								
<4	23	20	3	0.65	23	12	7 (4)	0.04*
≥4	3	2	1		3	3	0	

*p<0.05

Table.1.1.2 Correlations between RANK / RANKL expression and clinicopathological variables. RANK expression was found to be related to age (p=0.007), however the other clinical variables were not significantly correlated with RANK expression. All the variables were not correlated with RANKL expression except the number of OCs. *Significant difference p<0.05.

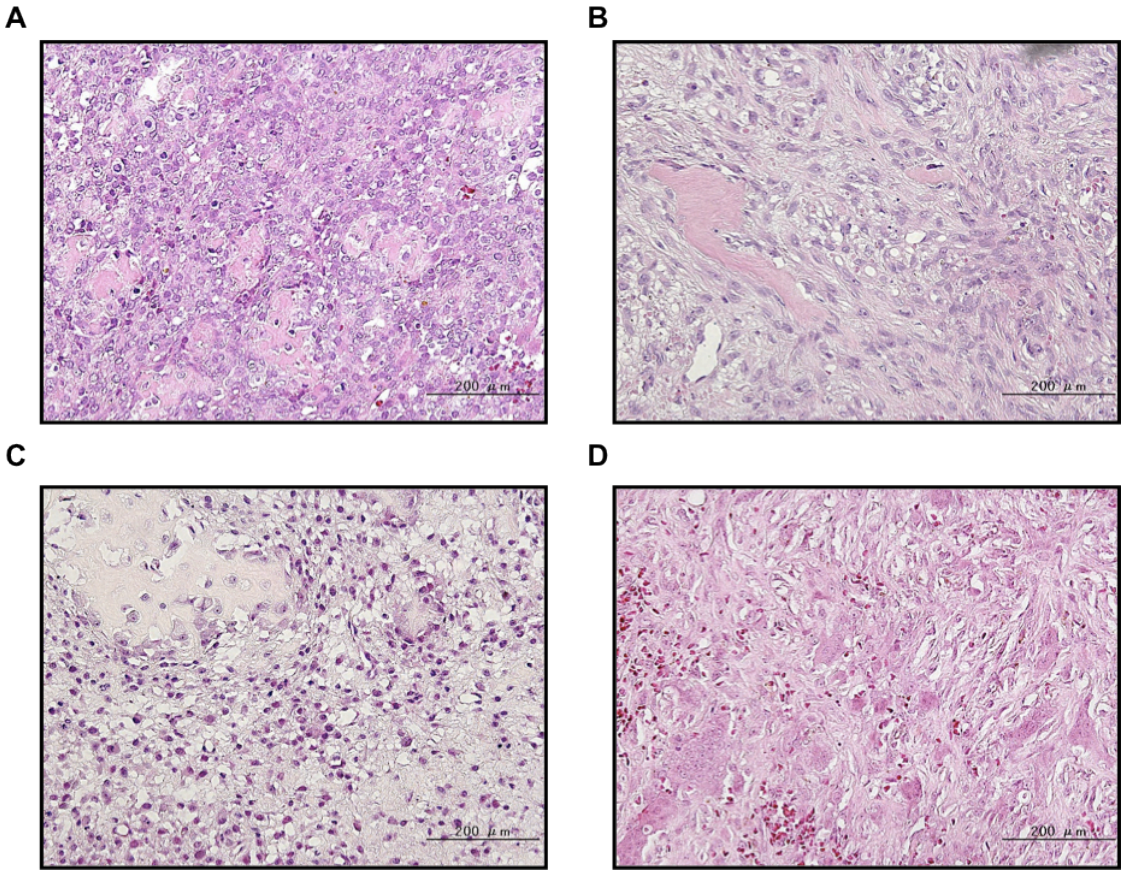

Fig.1.1.1 Histopathological analysis based on HE staining.

Typical OSA subtypes were classified as (A) osteoblastic, (B) fibroblastic, (C) chondroblastic and (D) giant cell type (x200).

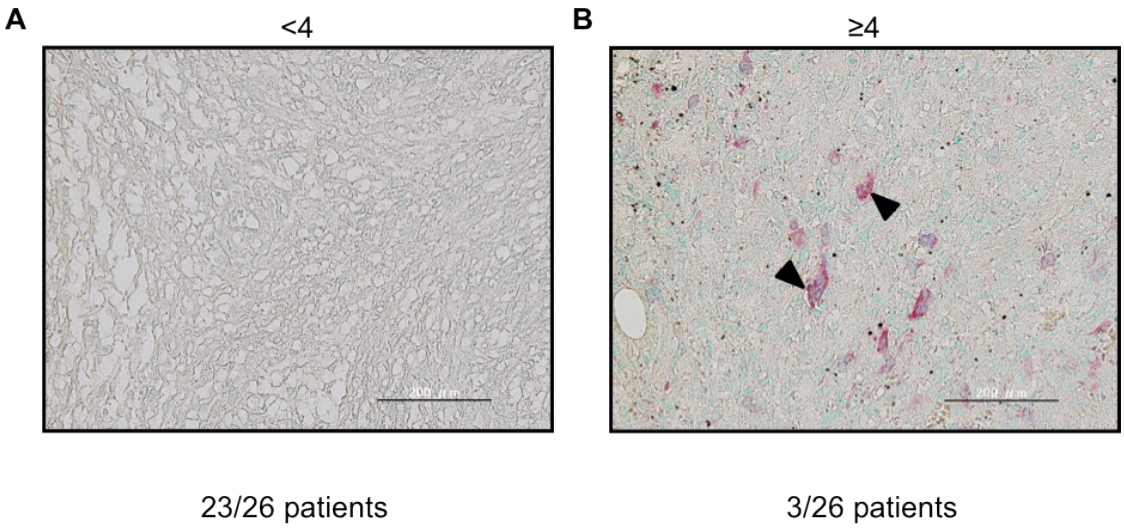

Fig.1.1.2 Typical findings of TRAP-positive cells on OSA patients and OC numbers were calculated as <4 or ≥ 4 (x200). Arrowheads indicating TRAP positive OC. Twenty-three of 26 OSA patients showed <4 (A), and remaining 3 showed ≥ 4 (B). There were no correlations to clinical variables including OSA subtypes.

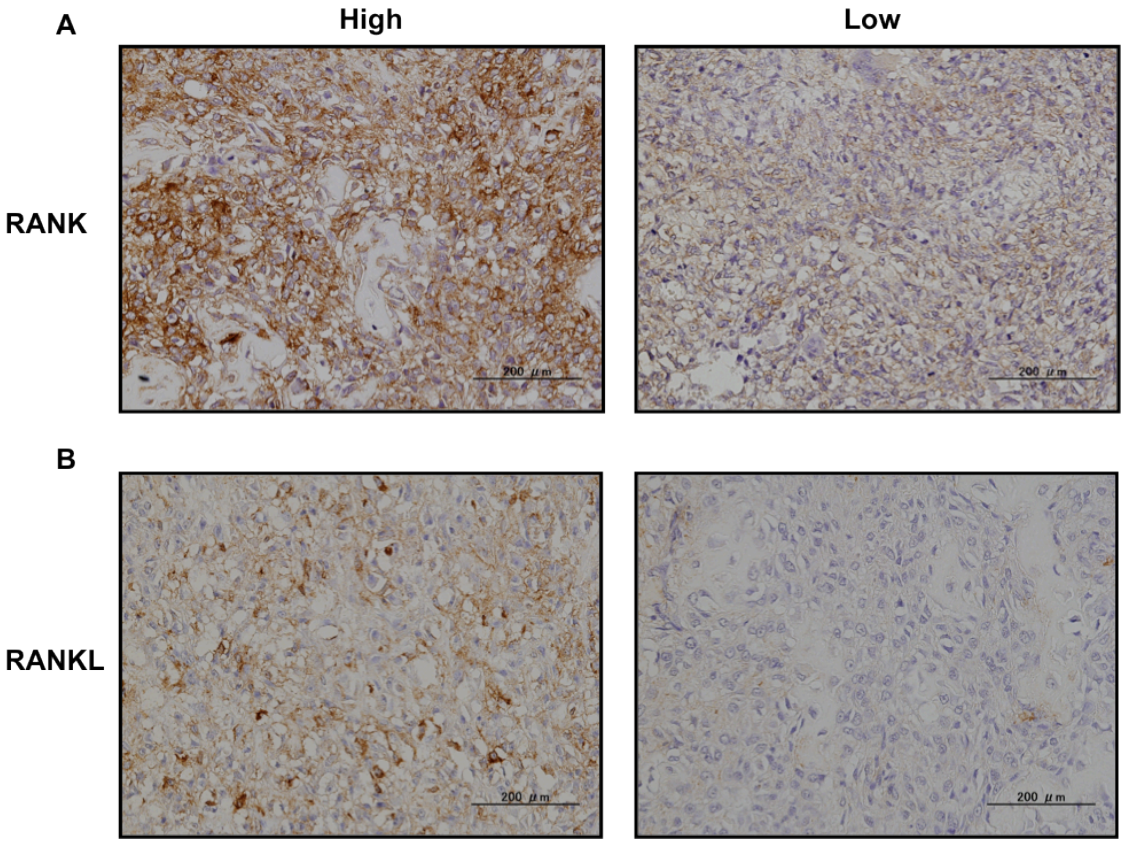

Fig.1.1.3 Representative of histopathological findings of high and low expression of RANK and RANKL on IHC in OSA patients. (A) showed RANK expression, (B) showed RANKL expression (x200).

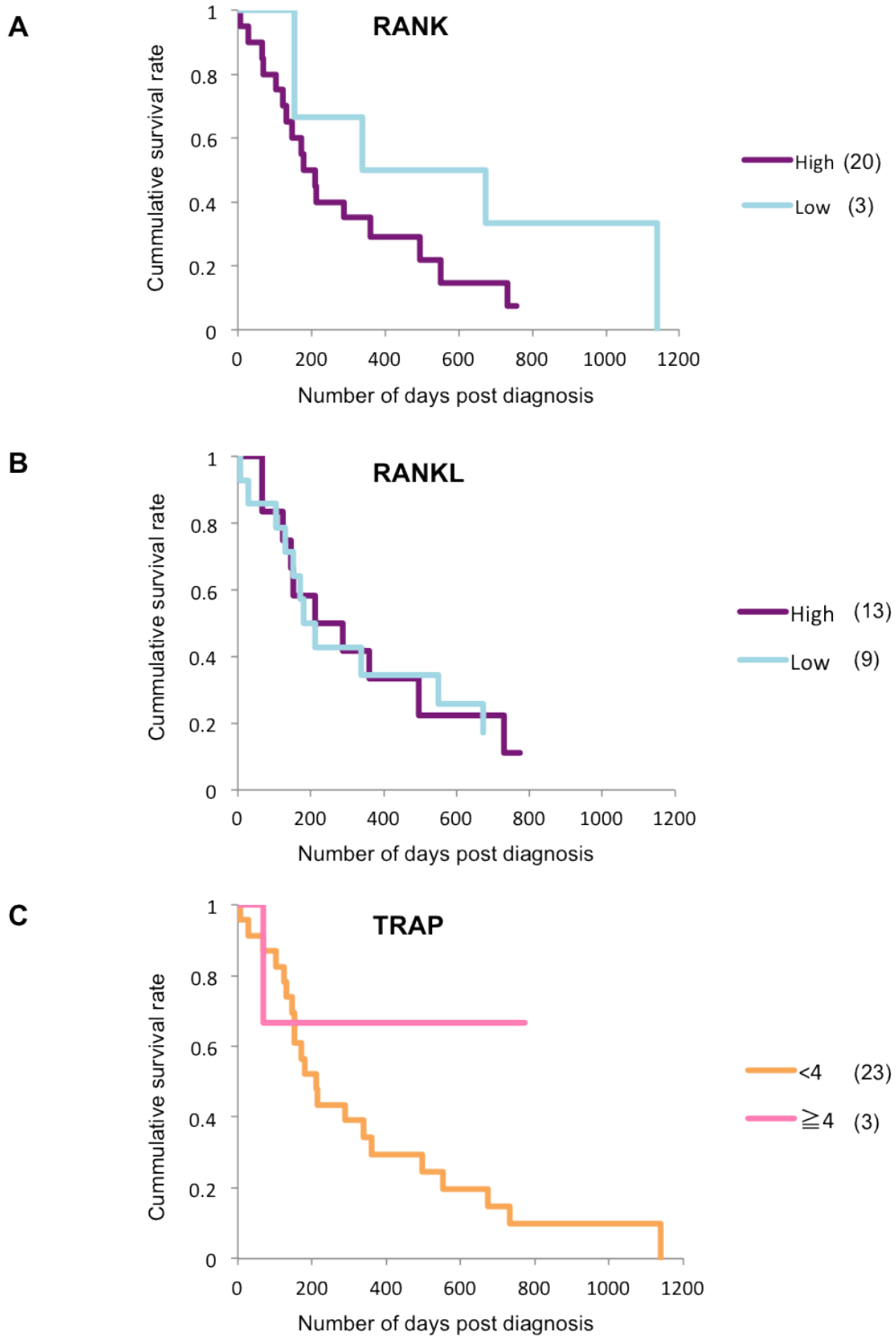

Fig.1.1.4 Kaplan-Meier survival time of patients with high and low expressions of RANK and RANKL (A, B), and with the number of TRAP-positive OCs (<4 and ≥ 4)(C). There was no significant difference between the expression levels of RANK, RANKL and TRAP in canine OSA patients.

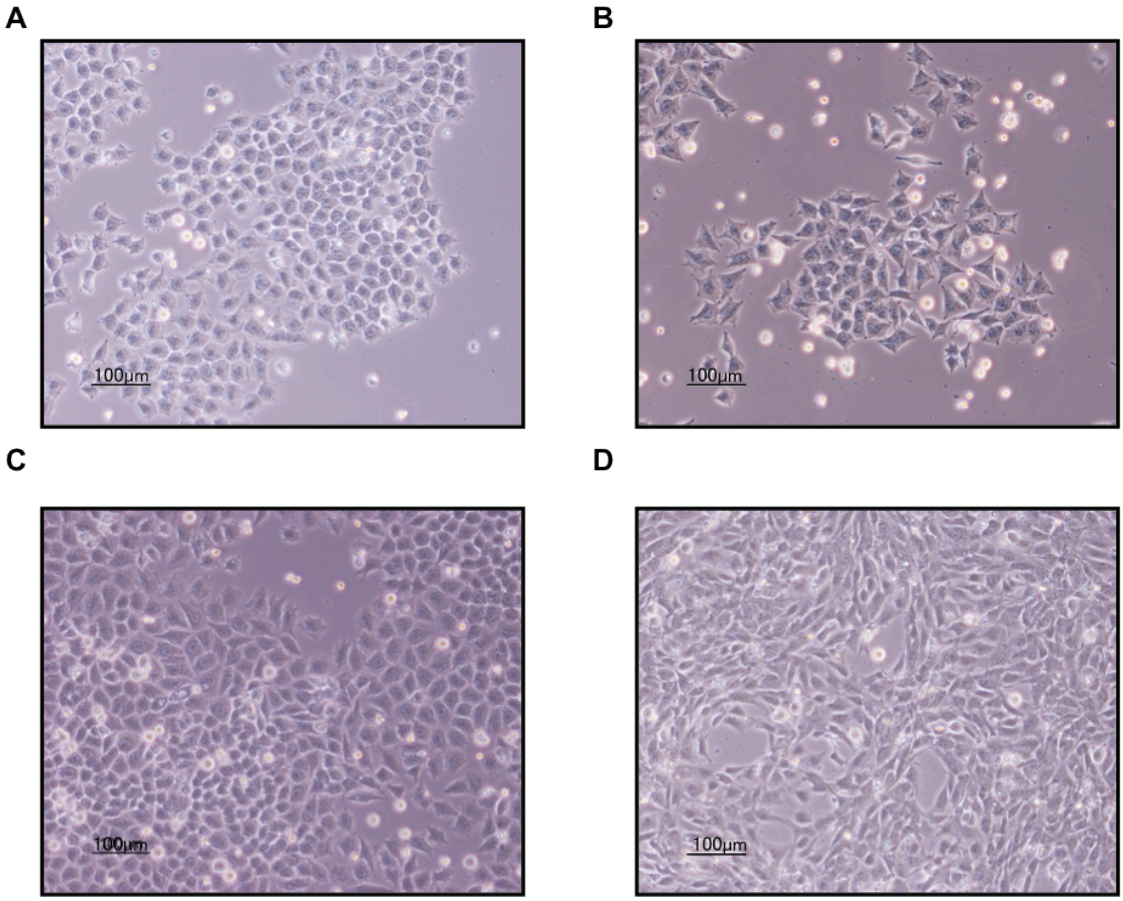

Fig.1.1.5 The morphology of canine OSA cell lines used in this study. (A) HMPOS showed polygonal morphology; (B) POS showed mixed with spherical, fibroblastic and polygonal cells; (C) OOS consisted of spherical cells, fibroblast-like cells, polygonal cells and multinucleated giant cells; (D) CHOS was fibroblastic type.

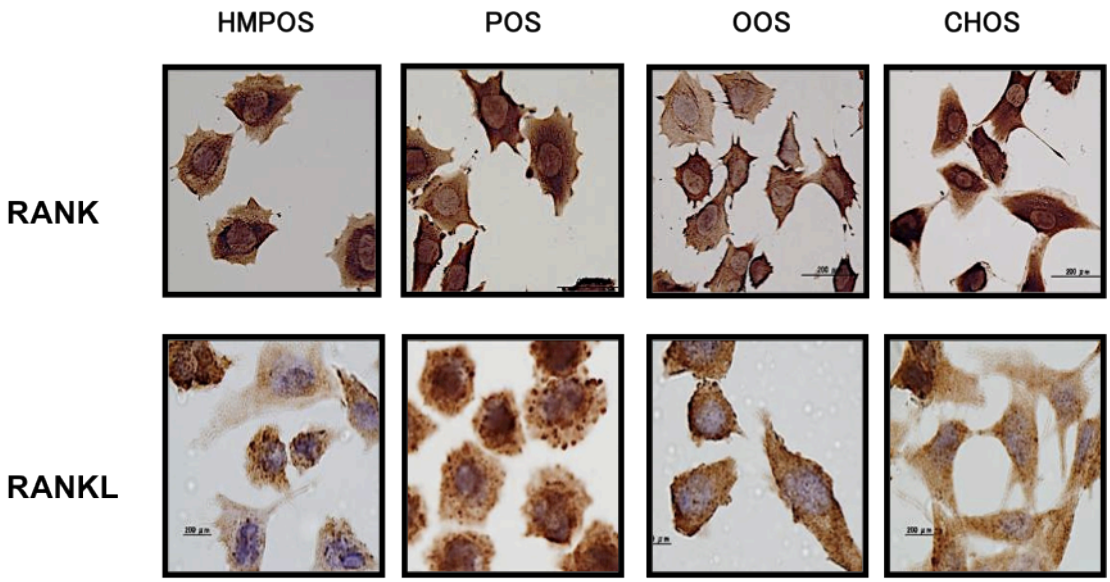

Fig.1.1.6 Immunocytochemistry revealed that RANK and RANKL proteins were expressed on both the cell membrane and cytoplasm of all OSA cell lines.

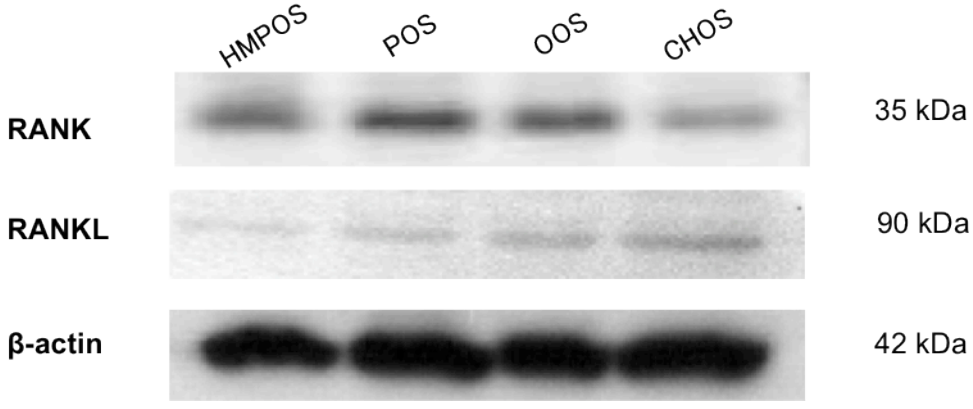

Fig.1.1.7 WB analysis for 4 OSA cell lines. RANK protein was expressed in all cell lines. The highest expression was observed in POS, followed by OOS,HMPOS and CHOS in order. RANKL protein was expressed in all cell lines and the highest expression was observed in CHOS, followed by OOS, POS and HMPOS in order.

	HMPOS	CHOS
1 week	0	0
3 weeks	1.4 ± 1.6	0
5 weeks	38.6 ± 20.3*	0

Table.1.2.1 Number of lung metastatic nodules. Nude mice xenografted with HMPOS revealed metastatic nodules at the 3rd week, and at the 5th week, numbers of nodules were significantly increased (p<0.05). In nude mice xenografted with CHOS, there were no visible nodules throughout the observation period. *Significant difference p<0.05.

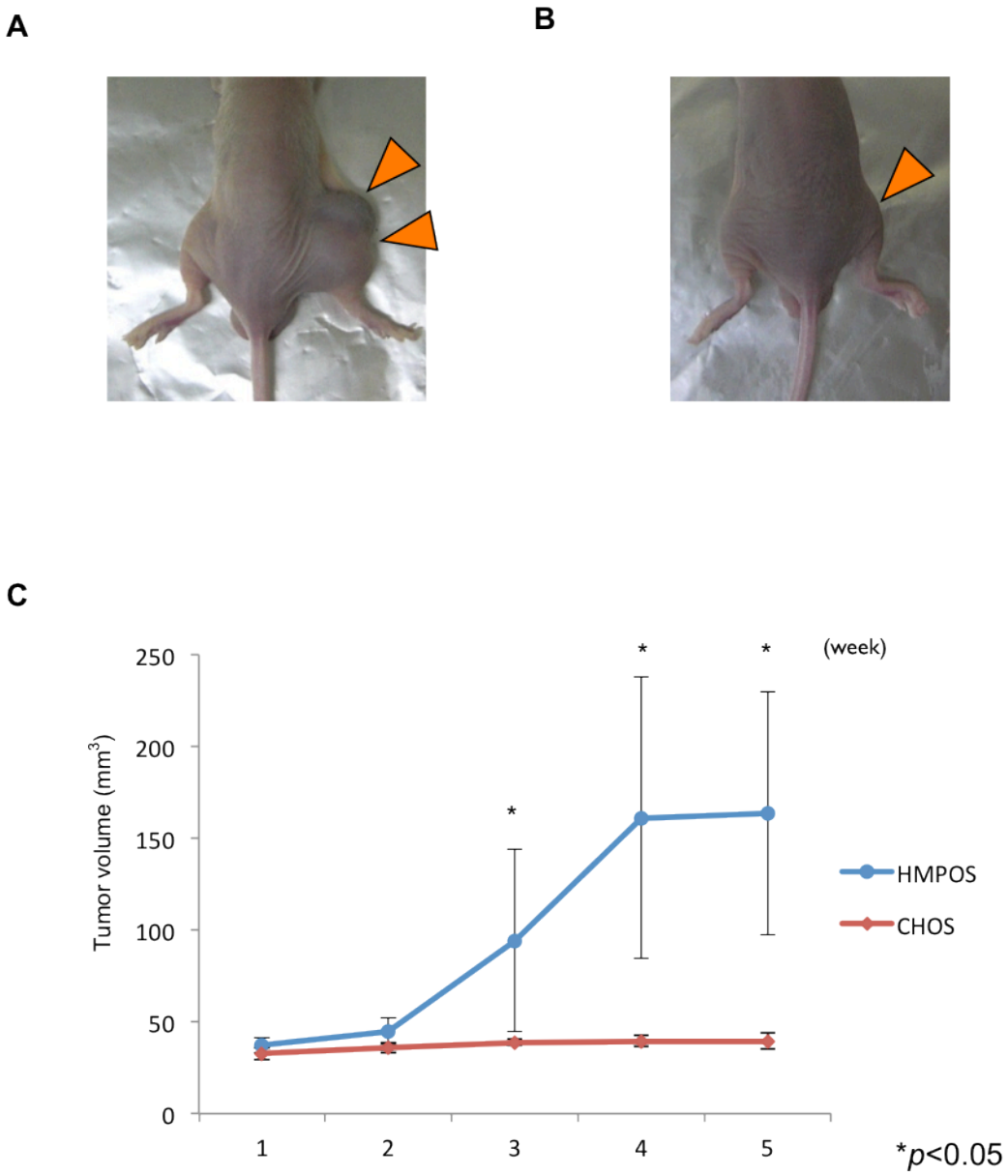

Fig.1.2.1 Tumor volume at the tibia was measured every 3 days after transplantation. (A), (B) represented transplanted site of HMPOS and CHOS, respectively. (C) Tumor volume of nude mice xenografted with HMPOS showed a significant increase, while in those with CHOS, tumor volume did not significantly increase. * represents a significant difference compared to those of the 1st week (p<0.05); vertical bars represents SD.

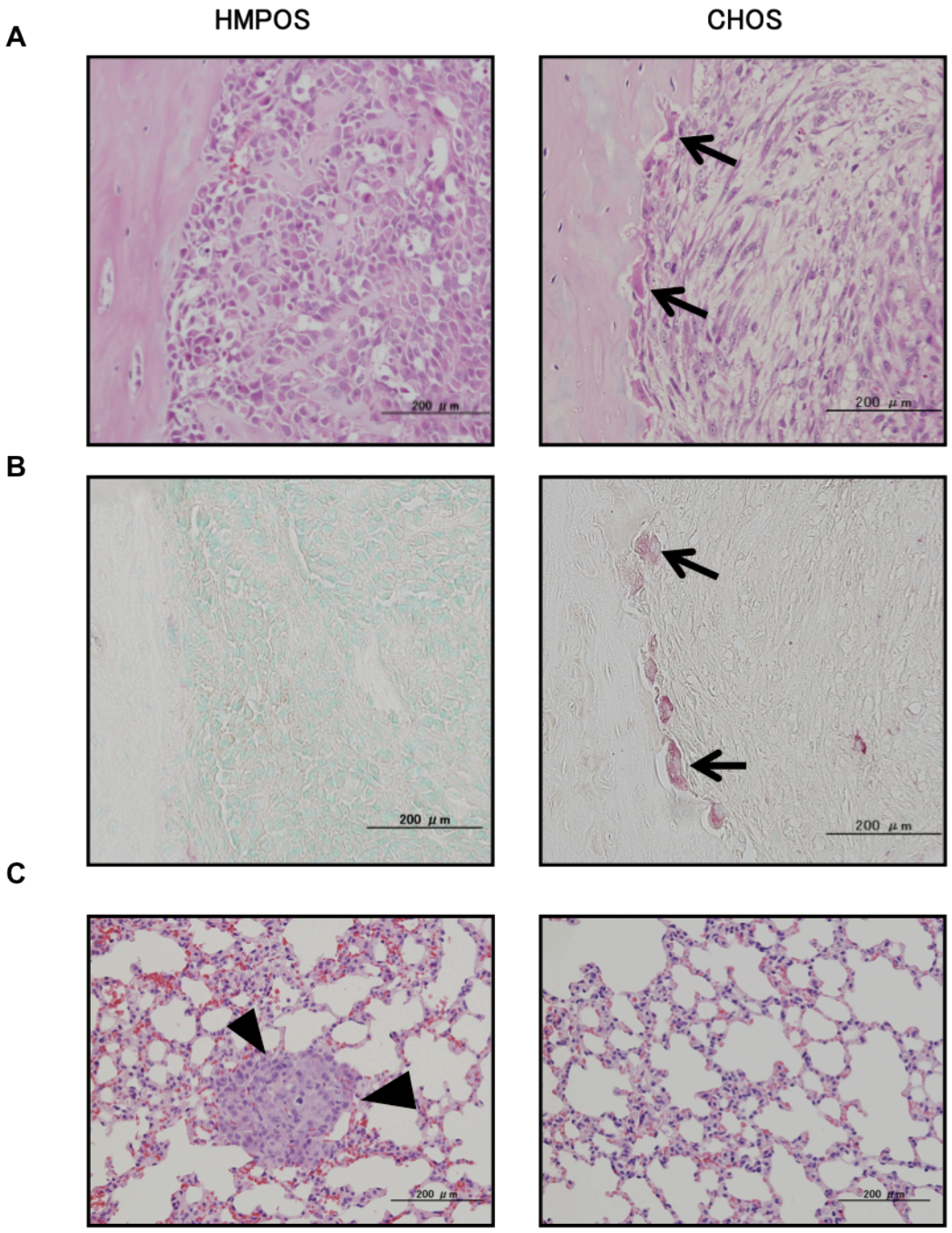

Fig.1.2.2 Histopathological analysis on the primary site of HMPOS- and CHOS-xenografted mice. (A) There were not apparent multinucleated cells at the interface of the tumor and bone cortex in HMPOS-xenografted mice, while clear multinucleated cells at the interface were observed in CHOS-xenografted mice (arrows). (B) TRAP staining confirmed that multinucleated cells to be TRAP-positive osteoclasts. (C) Metastatic nodules were observed only in a HMPOS-xenografted mouse (arrowheads).

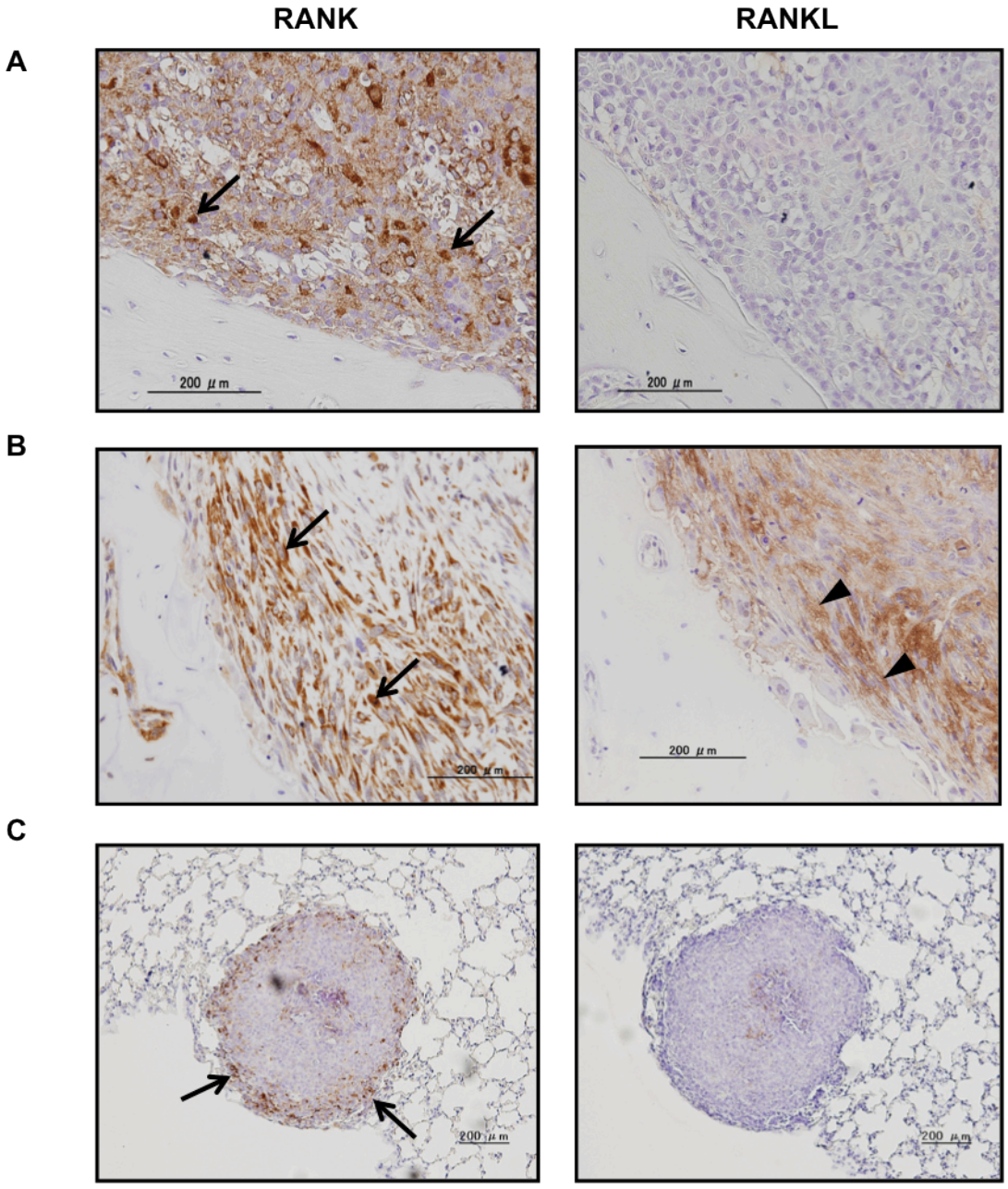

Fig.1.2.3 IHC on the primary lesions of HMPOS-xenografted and CHOS-xenografted mice, and metastatic nodules in HMPOS-xenografted mice. (A) RANK was clearly expressed on all the primary lesions developed in HMPOS-xenografted mice (arrows), while RANKL was negative during all the observation periods. (B) Primary lesions in CHOS-xenografted mice clearly showed the expression of both RANK (arrows) and RANKL (arrowheads). (C) RANK was only positive at the marginal area of the metastatic nodule (arrows), while RANKL expression was negative. Lung metastasis was not observed in CHOS-xenografted mice.

Fig.1.2.4 μ-CT findings of the tibia. (A) HMPOS-xenografted mice showed destruction of the tibial cortex and invasion to the bone marrow at the 3rd week. At the 5th week, tumor growth was aggressive and destroyed epiphyseal region (arrows) and extended to the outside of the tibia. (B) CHOS-xenografted mice showed osteolysis (arrow heads) at the 3rd week and the lesion became larger at the 5th week. The lesion seemed to show osteolysis of the bone cortex without invasion into the surrounding tissues.

Chapter 2

Function of RANK expression on canine OSA cell lines

Introduction

There have been several reports on RANK expression on tumor tissues such as breast cancer and primary bone tumor. Jones et al. (2006) reported that migration and metastasis of RANK-positive human epithelial cancers cells were regulated by RANKL. They suggested the important role of RANK-RANKL in cell migration and the metastatic behavior of cancer cells (Jones et al., 2006).

Furthermore, Mori et al. determined the expression of RANK on tissues from human OSA patients and reported that RANKL induced phosphorylation of extracellular signal-regulated kinases 1 and 2 (ERK1/2), p38 and inhibitor of κB (IκB) on RANK-positive human OSA cells (Mori et al., 2007). Another report also confirmed that RANK-positive human OSA cells stimulated by RANKL induced cell migration via activation of protein kinase B (PKB/AKT) and ERK1/2 (Akiyama et al., 2010).

According to those accumulating studies, RANK-RANKL is proposed as promising therapeutic target as well as keys to understand metastatic potential of tumors. However, there are many other factors contributing to metastatic potential of OSA such

as ezrin, a member of the ezrin-radixin-moesin (ERM) proteins family (Khanna et al., 2004; Jaroensong T et al. 2011 in press) and metalloproteinases (MMPs) (Lana et al., 2000; Loukopoulos et al., 2004) .

MMPs are a family of proteolytic enzymes largely responsible for controlling degradation of extracellular matrix (ECM) (Bode et al., 1999). MMPs are classified into 6 subgroups depending on domain components, substrate specificity and sequence similarity (Snoek-van Beurden and Von den Hoff, 2005) as follows; collagenages (MMP 1, 8 and 13), gelatinases (MMP 2 and 9), stromelysins (MMP 3, 10 and 11), matrilysins (MMP 7 and 26), membrane type MMPs (MMP 14, 15, 16, 17, 24 and 25) and others. The gelatinases are known to be associated with invasion, metastasis and poor prognosis in highly metastatic human neuroblastoma (Sugiura et al., 1998). Additionally, MMP 2 and 9 are the two major MMPs involved in tumor invasion and metastasis in canine OSA (Lana et al., 2000; Loukopoulos et al., 2004). It is also known that osteoblasts produce various MMPs (MMP 2, 3 and 13) in bone microenvironment and these MMPs are essential for bone resorption together with enzymes produced by OCs (Kusano et al., 1998; MacDougall and Matrisian, 1995).

The gelatinases mainly digests gelatin and type Ⅳ collagen (major component of the basement membrane). The type Ⅳ collagen was also cleaved by other MMPs such as collagenases, gelatinases, stromelysins and matrilysins.

According to the result obtained in Chapter 1, RANK expression was observed on 88.4% of tissues of canine OSA patients and all 4 canine OSA cells. WB analysis revealed that RANK protein was expressed relatively higher in POS, then OOS, HMPOS and CHOS in order. Furthermore, in the xenograft mouse model in Chapter 1, HMPOS-xenografted mice showed aggressive tumor growth and high potential to lung metastasis, whereas CHOS-xenografted mice was the least malignant and slow proliferation rate. Thus these 2 cell lines were selected in this experiment.

The aim of this Chapter was to determine the function of RANK-expressing canine OSA cell lines. The signal transduction pathway, migration and invasiveness via RANKL stimulation were determined in HMPOS and CHOS cells. Additionally, certain MMPs mRNA expressions were analyzed to evaluate correlation to invasiveness of RANK-positive canine OSA cell lines under RANKL stimulation.

Materials and Methods

Cell culture

HMPOS and CHOS cell line were cultured as described in Chapter 1.

Western blot

Protein lysates were made from each cell line after 24 hours of serum starvation at 70-80% confluence as previously described in Chapter 1, and subjected to subsequent signal transduction analysis.

Signal transduction analysis

The signal transduction analyses were performed according to the previous report (Mori et al., 2007). Briefly, OSA cell lines were cultured for 24 hours in serum-free RPMI-1640. The cells were then cultured in the absence or presence of 100 ng/ml RANKL (R&D systems) for 5,15 and 30 minutes. Then, OSA cells were lysed as described in Chapter 1.

The level of phosphorylated (p-) and total forms of extracellular signal regulated kinase 1/2 (ERK 1/2), JNK, p38 and IκBα were detected by using specific antibodies (p-p38, p38, p-JNK, JNK, p-ERK 1/2, ERK1/2, p-IκBα; Cell Signaling Technology, Danvers, MA, USA., IκBα, c-Fos; Santa Cruz). Dilutions for p-p38, p38, p-JNK, JNK, p-ERK1/2, ERK1/2 and IκBα were 1:1000, and those for p-IκBα and c-Fos were at 1:200.

Transwell migration and invasion assay

To evaluate the relationship between RANKL stimulation on RANK-positive cells and metastatic potential of the cell lines, motility and invasiveness were analysed by using transwell migration and invasion assays. HMPOS and CHOS cells were detached and re-suspended in FBS-free RPMI-1640 medium at 80-90% confluent. For migration assay, $2.5x10^4$ cells in 500 μl volume were plated on the top chamber with a non-coated polycarbonate membrane with 8.0 μm pore size (BD Bioscience, Bedford, MA, USA) in triplicate, under absence of RANKL (control) or presence of 100 ng/ml RANKL. RPMI-1640 medium with 10% FBS was added in the lower chamber as a chemoattractant. After incubation for 24 hours, the cells migrated to the lower surface

of the polycarbonate membrane were fixed with methanol for 1 minute, followed by Wright-Gimza staining for 15 minute. The cells, which did not migrate through the pores, were mechanically removed by cotton swab moistured with the medium. The mean number of migrated cells was counted in random 5 fields of each membrane at 100 x magnification.

The invasion assay of the HMPOS and CHOS cells was also performed by using Matrigel-coated transwell inserts polycarbonate membrane of 8.0 μm pore size (BD Bioscience). The procedure was followed after the migration assay. After Wright-Gimza staining, the mean number of migrated cells was counted from 5 random fields of each membrane at 100 x magnification.

Real-time migration and invasion monitoring

The xCELLigence system (Roche Diagnostics) was used to measure real-time migration and invasion monitoring according to the manufacture's instruction. This system is to measure the change in electrical impedance as cells pass through the upper chamber to the lower chamber. The bottom of the upper chamber is covered by a

microelectrode, so that when cells attach and spread over the electrode, electrical impedance increases. The electrical impedance is converted to the dimensional parameter called Cell Index (CI), which reflects the integrated cellular statues in the culture.

Using the CIM-Plate 16 (Roche Diagnostics) and xCELLigence System RTCA DP Instrument, $5x10^4$ cells were seeded onto each upper chamber of a CIM-Plate 16 with non-FBS containing medium under absence or presence of either 50 ng/ml or 100ng/ml RANKL. For the invasion assay, the upper chambers were coated with Matrigel diluted with 1:40 with FBS-free medium. The upper chamber was then placed on the lower chamber of the CIM-Plate 16 containing growth medium supplemented with 10% FBS as a chemoattractant. Cell migration and invasion were monitored for up to 24 hours, and CI values were analyzed by RTCA software version 1.2.

RNA extraction and quantitative RT-PCR analysis

MMPs are involved in degradation of Matrigel components (laminin and collagen Ⅳ). To clarify the effect of RANKL on OSA invasion via MMPs, collagenase (MMP13), gelatinase (MMP2, 9) and matrilysins (MMP7) were selected in this study. The mRNA expressions of these MMPs were measured by qRT-PCR.

Cells were cultures under absence or presence of 100 ng/ml RANKL and total RNA was extracted from each cell line using RNeasy Mini kit (Quiagen) according to the manufacturer's instructions. Complementary DNA was synthesized from 1 μg of total RNA with Quantitec Reverse Transcriotion (Quiagen, Hilden, Germany). qRT-PCR was carried out by ABI prism 7900 (Applied Biosystems, Tokyo, Japan). The specific primers for MMP2, 9, and 13 were used from the previous report (House et al., 2007), and designed by primer 3 software for MMP7 (Table.2). The relative expression of each gene was calculated as the ratio to RPL32. Three step qRT-PCR was subjected for MMP2, 7 and 9, then started at 95℃ for 10 minutes, repeating 40 cycles of denaturation at 94℃ for 10 seconds, annealing at 58℃ for 20 seconds and enlogation at 72℃ for 30 seconds. For MMP13, two step qRT-PCR was used; at 95℃ for 10

minutes, followed by repeating 40 cycles at 95℃ for 5 seconds and at 60℃ for 30 seconds. A dissociation curve analysis was performed after final amplification. Using the complementary DNA, PCR was carried out and run electrophoresis to see expression pattern as well as to confirm single bands.

Statistical analysis

The mean and SD of the number of migrated and invaded cells were calculated. The statistical comparisons for the number of cells and expressions of each MMP markers were made by using Student's *t*-test. $P<0.05$ was considered as statistically significant.

Results

Signal transduction pathways under RANKL stimulation

Fig.2.1 shows the WB analysis for molecules in the RANKL-induced signal transduction pathways in RANK-positive OSA cell lines. RANKL induced phosphorylation of ERK1/2 in a time-dependent manner in both HMPOS and CHOS cell lines. In HMPOS cell line, the phosphorylation of ERK 1/2 reached to the peak at 15 minutes after RANKL stimulation and returned to the original level at 30 minutes, while CHOS revealed relatively higher expression at 5 minutes, then started to de-phosphorylate at 15 minutes. Additionally, the maximal phosphorylation of IκB was observed after 30 minutes in both HMPOS and CHOS cell lines. However, phosphorylation of JNK and p38 was not clearly appeared with weak signals and without time-dependent manner. Moreover, expression of c-Fos remained the similar level after RANKL stimulation.

Migration and invasion of OSA cell lines after RANKL stimulation

Fig.2.2 shows the results of migration and invasion assay using the transwell assay. In HMPOS cell line, the number of migrated cells was significantly increased after RANKL stimulation (p=0.033), while in CHOS cell line there was no significant increase after stimulation (p=0.300). The number of invaded HMPOS cells significantly increased after RANKL stimulation (p=0.0023), while a significant decrease in invasion was observed in CHOS cell line (p=0.035) (Fig.3.2B).

Fig.2.3 shows the real-time monitoring of migration and invasion of HMPOS and CHOS cells after RANKL stimulation. Similar to the result from transwell assay, migration of both HMPOS and CHOS was increased under the presence of RANKL. In HMPOS, there was a significant difference between the control and 100 ng/ml RANKL stimulation. Furthermore, invasion was significantly increased in HMPOS, while decreased in CHOS cells by either dose of RANKL stimulation.

Expressions of MMPs associated with invasion of OSA cell lines

Fig.2.4 shows the expression pattern of MMPs under absence or presence of RANKL in HMPOS and CHOS cell lines. MMP2 were clearly enhanced in HMPOS after RANKL stimulation, while no clear change was observed in CHOS. MMP7 was only detected in HMPOS after RANKL stimulation. MMP9 was not determined in both cell lines. MMP13 expression showed an increase in both cell lines after RANKL stimulation.

Fig.2.5 shows the relative mRNA expression of MMPs under presence or absence of RANKL by qRT-PCR. There was a significant increase in MMP 2 mRNA after RANKL stimulation in both HMPOS (p=0.0074) and CHOS cell lines (p=0.0011). MMP 7 was significantly increased in HMPOS after the stimulation (p=0.0054), while its expression was not detected in CHOS. The expression of MMP 9 was not detected in both HMPOS and CHOS. The expression of MMP 13 was significantly reduced in HMPOS cells (p=0.042), while there was no statistical difference in its expression in CHOS cells.

Discussion

The experiments in this Chapter were aimed to determine the function of RANK-expressing OSA cell lines under RANKL stimulation. According to the result from Chapter 1, I confirmed the expression of both RANK and RANKL on canine OSA cell lines.

Mori et al. reported that RANK-expressing human OSA cells exhibited phosphorylation of ERK1/2, IκB and p38 with RANKL stimulation. They found that after stimulation with 50 ng/ml of RANKL, phosphorylation of ERK1/2, IκB and p38 was detectable at 2, 15 and 10 minutes, and the phosphorylation reached plateau at 5, 15 and 60 minutes, respectively (Mori et al., 2007). Another report also confirmed that RANK-positive human OSA cells with RANKL stimulation induced phosphorylation of PKB/AKT and ERK1/2, leading to cell migration (Akiyama et al., 2010). However, the involvement of these pathways in OSA pathophysiology was not identified.

In agreement to these reports, WB analysis for molecules of the signal transduction pathways of RANK-expressing HMPOS and CHOS cell lines demonstrated phosphorylation of ERK1/2 and IκB α in a time-dependent manner and

reached the peak at 5 and 30 minutes after RANKL stimulation. However phosphorylation of JNK and p38 was not detected in both HMPOS and CHOS cell lines. In addition, c-Fos, known as proto-oncogene and is necessary for murine OSA development (Wang et al., 1995), is also activated to form complex with activator protein 1 (AP-1) via RANKL stimulation through OCs differentiation (Wagner, 2002). However in this study, the activation of c-Fos in both HMPOS and CHOS remained stable under absence or presence of RANKL. Thus, ERK1/2 and IκB α may be the two main pathways involved in canine OSA cell lines under RANKL stimulation.

Furthermore, migration and invasion potential of HMPOS cell line significantly increased after RANKL stimulation. Although CHOS cell line showed no significant increase in migration after the RANKL stimulation, invasion potential was shown to reduce significantly after the stimulation. Since there is a report which shows potential of MMPs involvement in canine OSA metastasis and invasion (Lana et al., 2000; Loukopoulos et al., 2004), it is possible that change in migration and invasion of OSA cell lines under RANKL stimulation may be associated with the expression of MMPs.

The comparison of relative mRNA expression of MMPs under absence or presence of RANKL showed a significant increase in MMP 2 and a decrease in MMP 13, while MMP 9 was not detected in both HMPOS and CHOS cell lines. Interestingly, the expression of MMP 7 was detected only in HMPOS cell, and a significant increase was found after the stimulation.

MMP 2 and MMP 9 are major gelatinases, which are associated with invasion, metastasis and poor prognosis in human highly metastatic neuroblastoma and canine OSA (Lana et al., 2000; Sugiura et al., 1998). In addition, MMP 7 has a potential of generating RANKL to be an active soluble form that can promote OCs maturation and activation in human prostate cancer (Lynch et al., 2005). Moreover, MMP 13 is known to activate MMP 9 and associated with tumor-induced osteolysis observed in human breast cancer (Knauper et al., 1997; Nannuru et al., 2010).

In accordance with these reports, the increase of MMP 2 in both HMPOS and CHOS cell lines was well correlated with their migration potential. However, MMP 9 was undetected in both cell lines under absence or presence of RANKL. MMP 9 is mainly produced by OCs, thus OSA cell lines themselves are not participated in bone

resorbing activity. Furthermore, a decrease in MMP 13 under RANKL stimulation also suggested that MMP 9 expression was not activated through MMP 13 in these cell lines. However, based on the result from Chapter 1, although an increase of MMP 7 on HMPOS cell line was found under RANKL stimulation, HMPOS-xenografted mice did not induce active OCs at the interface of the tumor and bone. Moreover, the MMP 7 expression in CHOS cell line was not detected while CHOS-xenografted mice model induced OCs at the interface of the tumor and bone. These results were inconsistent to the literature on MMP 7 potential of generating RANKL from cells to promote osteoclastogenesis. The mRNA expression of MMPs may not be reflecting actual active form of MMPs, leading to the different phenomenon in *in vitro* and *in vivo*. Thus further analysis such as gelatin zymography assay should be required to confirm active forms of MMPs.

Similar to the previous reports (Akiyama et al., 2010), RANKL triggered the migration and invasion via ERK1/2 and IκB pathways in canine OSA cell lines, while activations of p-38 and JNK were not evident. Although p38 and JNK are belonged to MAPK family as ERK1/2, they may not be the major signal pathways in canine OSA

cell lines. According to the result from the xenograft mouse model established in Chapter 1, elevated MMP 2 and MMP 7 via activation of ERK1/2 and IκB may be correlated to metastatic potential of HMPOS. This result agreed with the report in human, which showed that high MMP 7-expression via ERK1/2 activation was correlated to its metastatic potential (Yue et al., 2009). Thus, MMP 2 and MMP 7 may be key MMPs to regulate migration and invasion of OSA cell lines.

Based on this study, I confirmed the function of RANK on OSA cell lines under RANKL stimulation and together with the results from Chapter 1, targeting RANKL produced by OSA cell lines could be a prominent therapy in dogs. To further understand the effect of RANKL-targeted therapy, *in vitro* and *in vivo* function of RANKL by canine OSA cell lines should be analyzed.

Table.2.1 Sequence of primers used for the real-time PCR

Gene	Forward primer (5' - 3')	Reverse primer (5' – 3')	Product size (bp)
MMP 2	AACTACAACTTCTTCCCCCGA	GGGAACTTGCAGTACTCTCC	382
MMP 7	GATGTGGTGTGCCTGATGTC	CTCCTCTTGCAAAGCCAATC	228
MMP 9	GAGTTTCGACGTGAAGACGCAGAC	CAAAGGTCACGTAGCCCACTTCGT	200
MMP 13	AGGAGATGCCCATTTTGATG	TGGCATCAAGGGATAAGGAG	290
RPL 32	TGGTTACAGGAGCAACAAGAA	GCACATCAGCAGCACTTCA	100

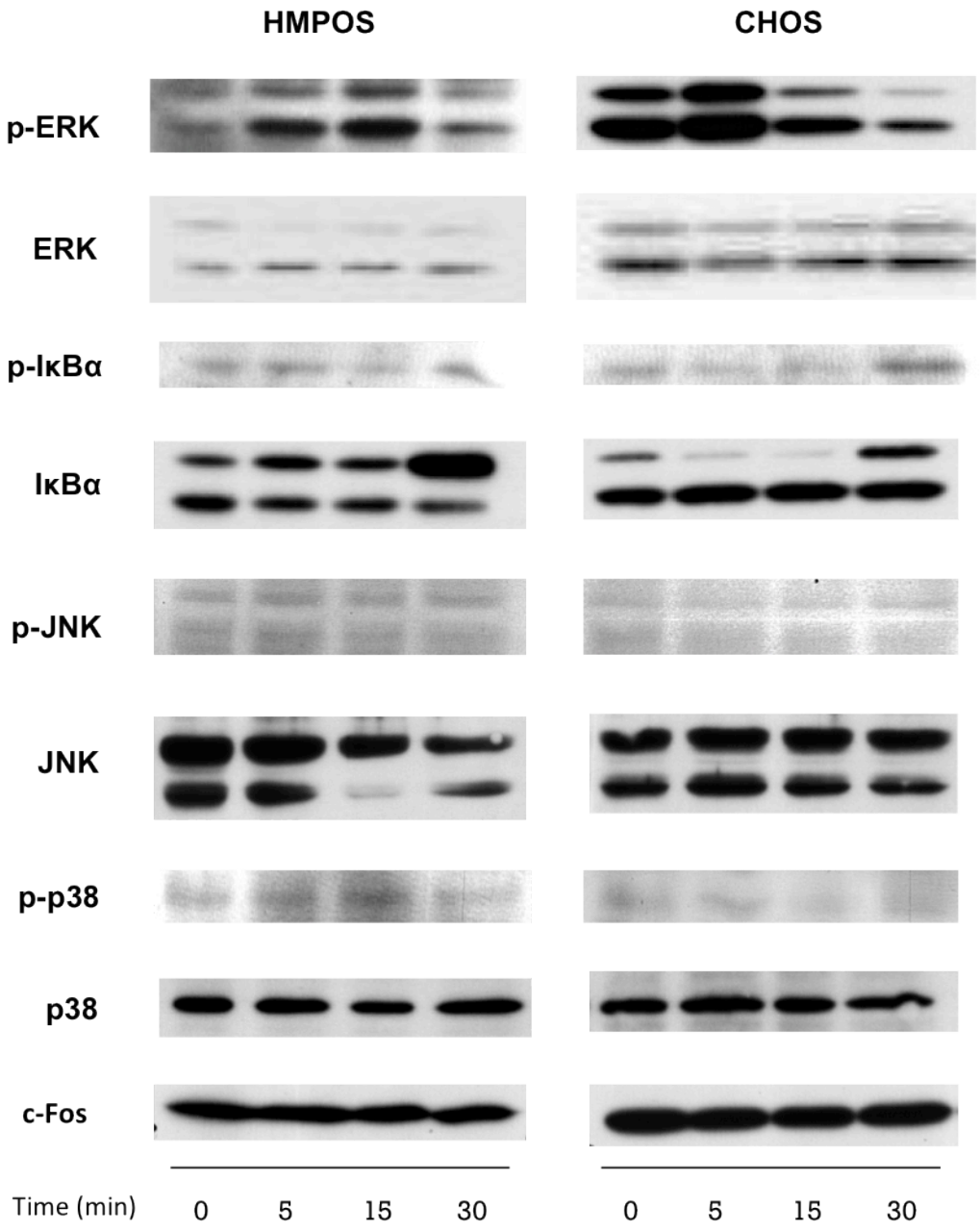

Fig.2.1 Signal transduction pathways after RANKL stimulation at 0, 5,15 and 30 minutes in HMPOS and CHOS cell lines. Both cells were serum-starved for 24 hours, then incubated at 5, 15 and 30 minutes under absence or presence of 100 ng/ml human RANKL.

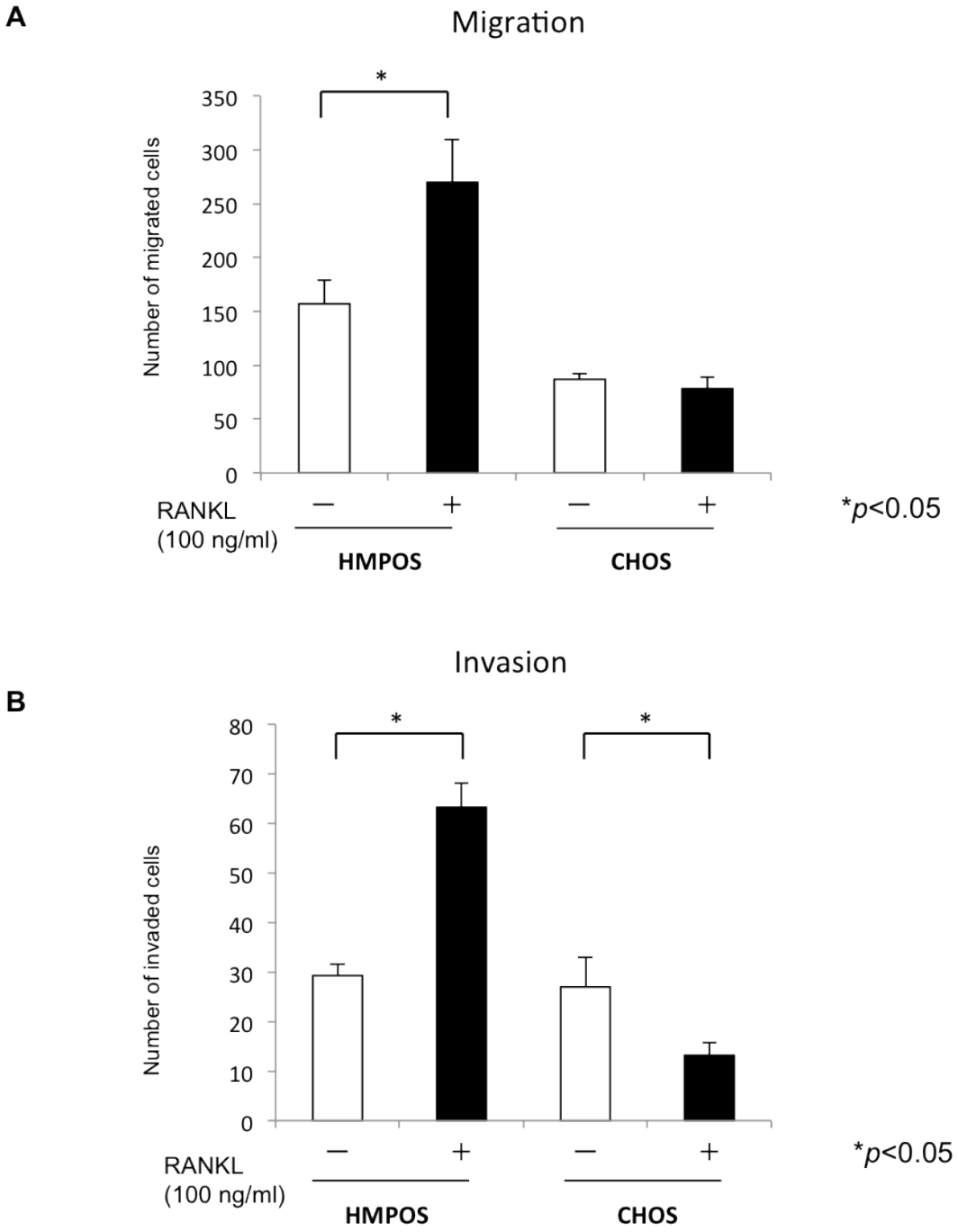

Fig.2.2 Migration and Invasion assay using the BD chamber method under absence or presence of 100 ng/ml RANKL for 24 hour. (A) There was a significant increase in number of migrated cells in HMPOS cells after RANKL stimulation, while no statistical difference was observed in CHOS cells. (B) RANKL stimulation induced a significant increase in number of invaded cells in HMPOS cells, while there was a significant decrease in invasion in CHOS cells.

* represented significant difference ($p<0.05$); vertical bars represents SD.

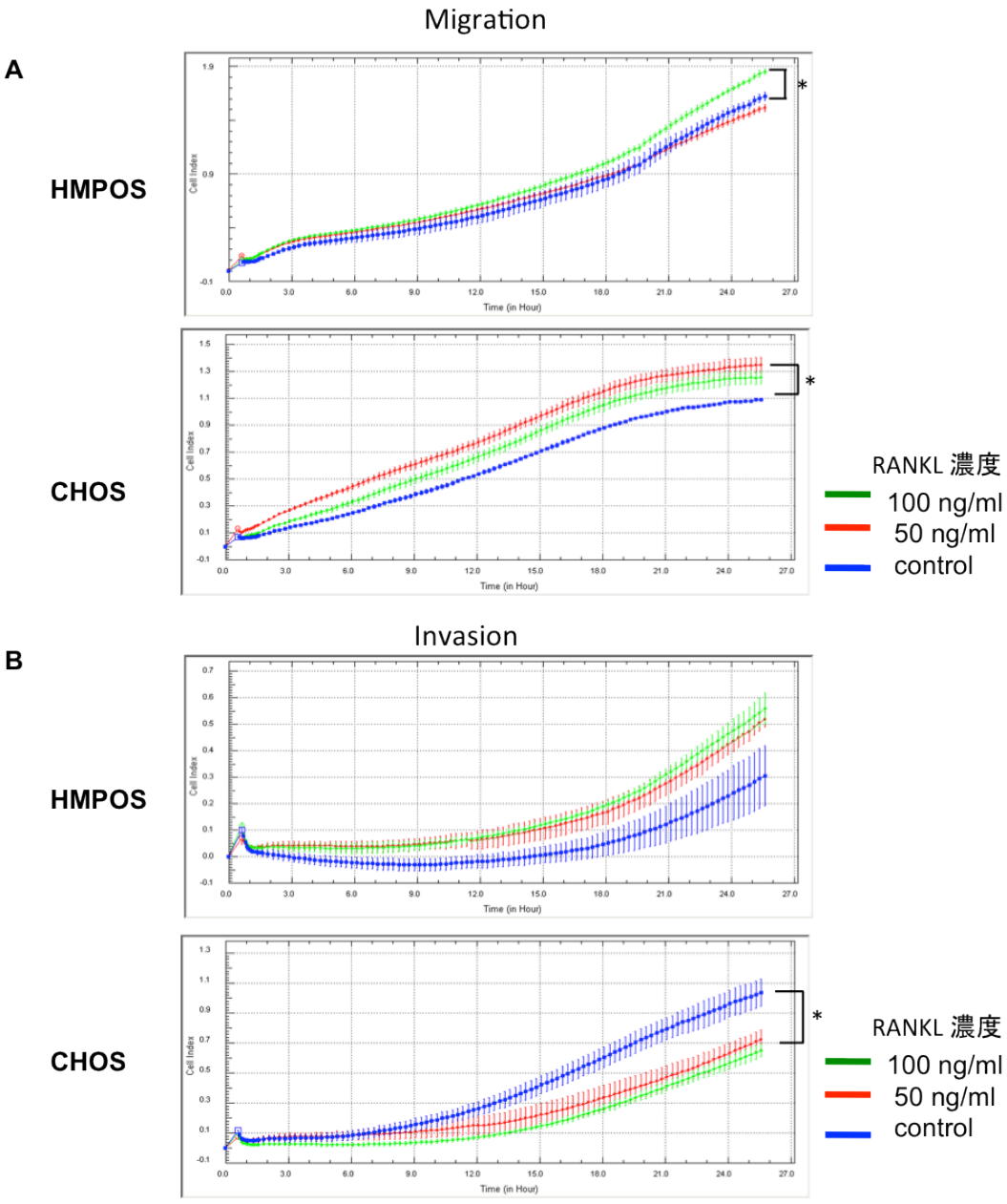

Fig.2.3 The effect of RANKL at 50 ng/ml and 100 ng/ml on real-time migration and invasion of HMPOS and CHOS cells by using xCELLigence system. (A) The significant increase in migration after 100 ng/ml (HMPOS) and 50 ng/ml (CHOS) RANKL stimulation. (B) In HMPOS, invasion potential seemed to increase after RANKL stimulation, whereas in CHOS, invasion potential was significantly decreased after RANKL stimulation at either dose. *Significant difference $p<0.05$

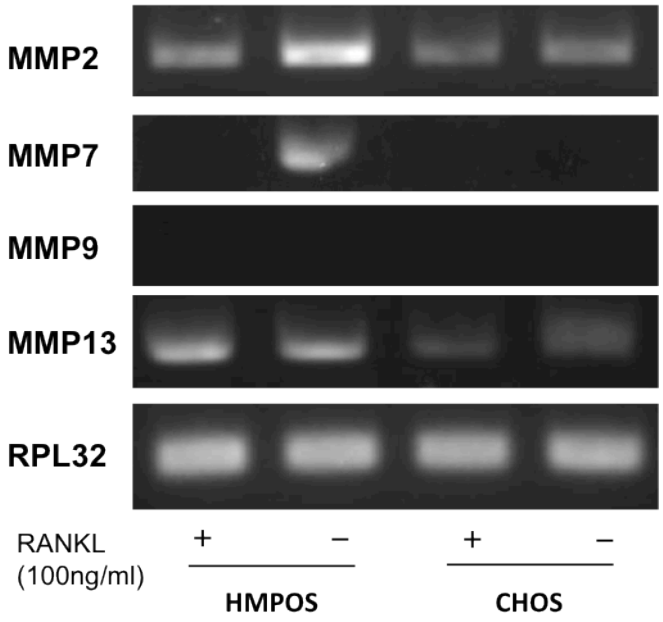

Fig.2.4 The expression pattern of MMPs in HMPOS and CHOS under absence or presence of RANKL. MMP2 were clearly enhanced in HMPOS after RANKL stimulation, while no clear change was observed in CHOS. MMP7 was only detected in HMPOS under presence of RANKL. MMP9 was not determined in both cell lines, MMP13 expression showed an increase in both cell lines after RANKL stimulation. Single bands for each MMP2, 7, 9 and 13 were confirmed.

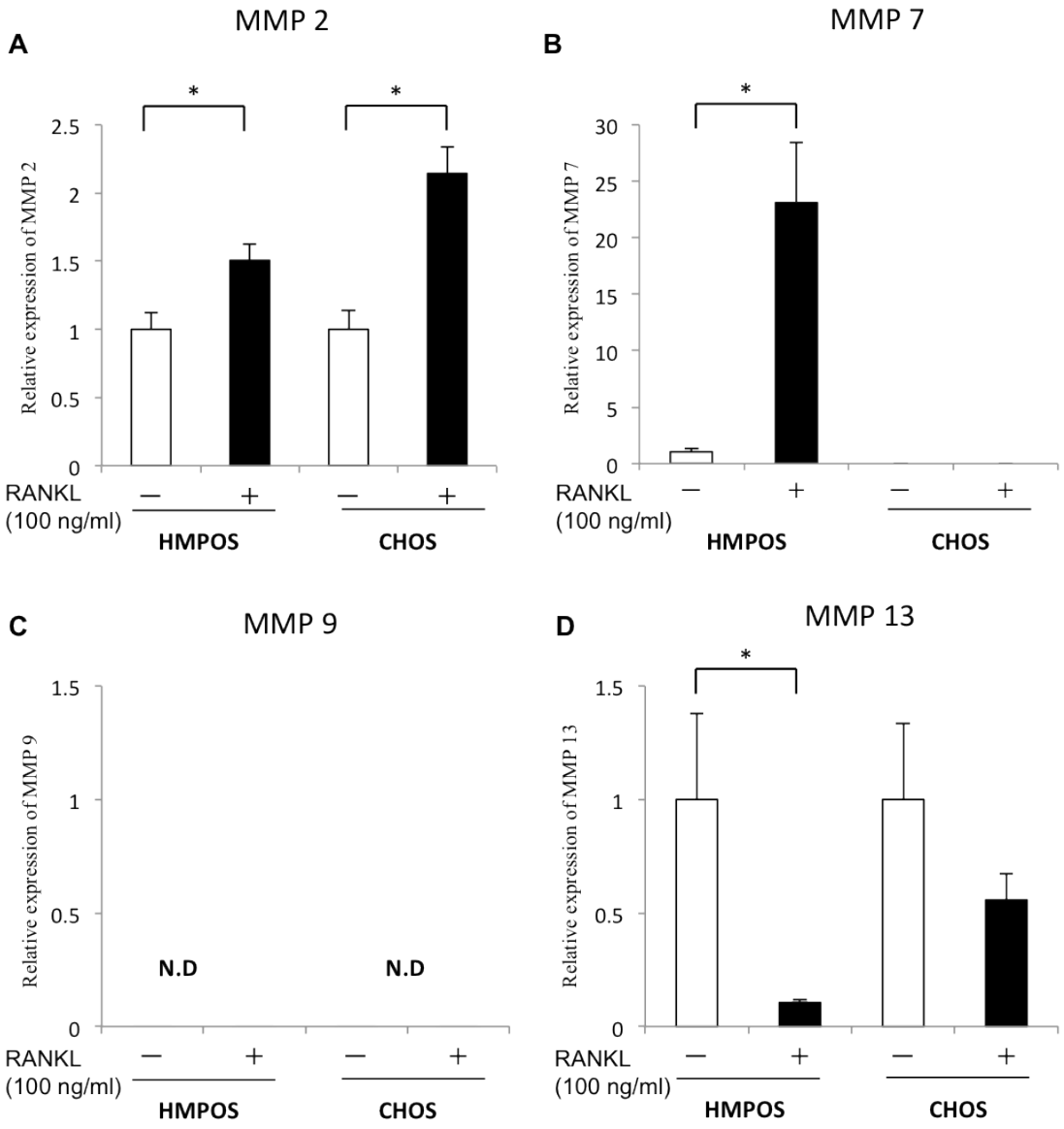

Fig.2.5 The comparison of relative mRNA expression of MMPs under presence or absence of RANKL (100 ng/ml) was analyzed by qRT-PCR. (A) There was a significant increase in MMP 2 after RANKL stimulation in both HMPOS (p=0.0074) and CHOS cell lines (p=0.0011). (B) MMP 7 was significantly increased in HMPOS cells after the stimulation (p=0.0054). (C) The expression of MMP 9 was not detected in both HMPOS and CHOS. (D) The expression of MMP 13 was significantly reduced in HMPOS cells (p=0.042), while there was no difference in its expression in CHOS. *Significant difference $p<0.05$; vertical bars represents SD.

Chapter 3

RANKL function in OSA cell lines and the effect of anti-RANKL antibody on the tumor growth in a xenograft mouse model

Introduction

There are accumulating evidences that OC formation and activity play a central role for tumor-induced osteolysis (Mundy, 2002; Roodman, 2004). OCs are primary cells for bone resorption and the *in vitro* method to determine differentiation of OCs is commonly used for understanding the OC-related diseases. Authentic OCs should fulfill the major criteria such as TRAP positivity, actin ring formation, and pit formation on dentine slices *in vitro*. Furthermore, RANK/RANKL are known as crucial factors for regulating OCs, thus targeting these molecules has attracted a great deal of interest with regard to treatment of bone tumors (Ando et al., 2008; Mori et al., 2009; Wittrant et al., 2004).

Bone metastasis is common in human breast cancer and prostate cancer patients with high incidence of significant skeletal-related events (SREs) such as hypercalcemia, pathologic fracture, and bone pain (Coleman, 1997). Therefore, palliative and anti-resorptive therapies are important not only to control the SREs, but also to obtain the quality of life. Based on this background, OCs-targeted therapies such as bisphosphonates and monoclonal anti-human RANKL antibody (denosumab®) are

promising modalities for bone metastatic tumors to suppress osteolysis and bone pain. Furthermore, Akiyama et al. (2008) and Mori et al. (2009) pointed out that primary bone tumor such as OSA could be a suitable candidate for OCs-targeted therapy. Since tumor cells themselves are unable to resorb bone matrix directly, OCs activity is prerequisite for invading bone and releasing bone-derived growth factors, which further promote tumor cells activation and progression by the consequence of bone matrix degradation. One study reported that RANK-Fc could suppress osteolytic lesions associated with human OSA development and local tumor growth in a mouse model (Lamoureux et al., 2008). Another recent report showed RANK-Fc suppressed migration and invasion of OSA cells and induced anoikis through inhibition of ERK. In addition, RANK-Fc inhibited bone resorption via suppression of OC formation and reduced metastatic nodules in human OSA cells-xenografted mice (Akiyama et al., 2010). There are still limitations and further studies are required in order to transfer this modality into the clinical use, however these data suggested the OCs-targeted therapy as a potential OSA therapy.

According to the result in Chapter 1, RANKL expression was found on canine

OSA cell line. Furthermore, the involvement of OCs in tumor-induced osteolysis was suggested in the xenograft mouse model using high-RANKL-expressing cell line (CHOS). Additionally, the function of RANK-expressing OSA cell lines was clarified in Chapter 2. Therefore, I hypothesized that RANKL-targeted therapy could be a promising treatment in canine OSA. The aim of this Chapter was to clarify the potential of osteoclastogenesis by canine OSA-producing RANKL using an *in vitro* OC differentiation method and to evaluate the effect of anti-mouse RANKL-neutralizing monoclonal antibody on the xenograft mouse model, in which the effect on skeletal lesions and direct antitumoral effect was investigated.

In the first section, I attempted to establish the OC differentiation method from canine bone marrow cells (BMCs) by using M-CSF and RANKL. Then, I investigated the effect of conditioned medium (CM) on OC formation by using the canine OC differentiation method. In the second section, the effect of anti-mouse RANKL-neutralizing monoclonal antibody was investigated by using CHOS-xenografted mice. In particular, the effect on tumor-induced osteolysis and tumor proliferation was focused.

Section 1: Diffrentiation of osteoclasts from canine bone marrow cells

Materials and Methods

Isolation of canine bone marrow cells (BMCs)

Healthy beagles were housed and cared under approval by the Animal Care Committee of the Graduate School of Agricultural and Life Sciences, the University of Tokyo. Canine BMCs were collected and cultured using the method previously reported (Isotani et al., 2006; Sago et al., 2008) with slight modifications. Briefly, under general anesthesia, 2 ml of bone marrow was aspirated from the proximal humeral condyle with a syringe containing 1000 IU/ ml of heparin sodium. BMCs were obtained by density gradient centrifugation at 450 x g using Ficoll (Sigma) for 30 minutes at 22℃. These preparations were then treated with hemolysis buffer (154 mM NH4Cl, 10 mM KHCO3, 0.1 mM EDTA) for 10 minutes to remove red blood cells, suspended in Cell Banker 1 (Wako) at a concentration of 2 x 10^7 cells/ml and stored in liquid nitrogen until further use.

OCs differentiation

OC differentiation was performed according to the culture method previously reported (Nagase et al., 2009) with minor modifications. Fig.3.1.1 shows the schematic diagram of osteoclastogenesis *in vitro*. BMCs in liquid nitrogen were thawed and washed with 10 ml of αMEM medium (Invitrogen) containing 10% FBS (Gibco BRL) and centrifuged at 300 x g for 5 minutes. They were then resuspended in αMEM containing 10% FBS and 100 ng/ml M-CSF (R&D systems, Minneapolis, MN, USA), seeded onto 10 cm-culture dishes（$1x10^7$cells/dish）, and incubated at 37ºC in a humidified atmosphere of 5% CO_2 (Fig.2.1.1 B). After 3 days of culture, the medium was changed in order to remove non-adherent cells, and the remaining cells were cultured for an additional 2 to 3 days. When cultures reached 70 to 80% of confluence, they were detached with 5x TE buffer (Sigma) and resuspended in αMEM containing 10% FBS and 10 ng/ml M-CSF under absence or presence of 100 ng/ml RANKL (WAKO). BMCs were then cultured at the concentration of 1.5 x 10^5 cells/well in 48-well plates for 1 to 4 days.

TRAP staining

Differentiated cells obtained were subjected to TRAP staining according to the method previously described（Suda et al., 1997）. Briefly, after aspiration of the medium, cells were fixed with 3.7% formalin for 5 minutes, washed with PBS (ph 7.4) twice and treated with acetone-ethanol (1:1) for 30 seconds. Then TRAP solution was added and incubated at 37ºC for 30 minutes, then counterstained with 0.1% brilliant-green for 5 minutes. TRAP-positive cells with 3 or more nuclei were counted.

Actin ring formation

Actin rings were stained with 0.3 μM rhodamine-conjugated phalloidin (Molecular Probes, Eugene, OR, U.S.A.), and the distribution of actin was detected using a fluorescence microscope (Biozero: KEYENCE, Osaka, Japan) as previously reported (Nagase et al., 2009; Suda et al., 1999).

Pit formation assay

Pit formation assay was performed according to the protocol previously

described (Miyazaki et al., 2000). Briefly, BMCs were cultured on dentin slices at the concentration of 1.5 x 10^5 cells/well in 48-well plates. At the end of the differentiation period, the medium was aspirated and 1 M NH_4OH was added to each well. Adherent cells were removed from dentine slices by ultrasonication. Resorption pits were stained with 0.5% toluidine blue, washed with distil water and visualized under the microscope.

Quantitative real time PCR

The mRNA levels of OC-specific markers (NFATc1, Calcitonin-R, RANK, and MMP9) were determined by quantitative real-time PCR (qRT-PCR). Total RNA was extracted from cells before RANKL stimulation, and 2 and 4 days thereafter, using of ISOGEN (Nippon Gene, Toyama, Japan) according to the manufacture's instructions. Complementary DNA was synthesized from 1 μg of total RNA and the products were subjected to qRT-PCR as previously described in Chapter 2. The specific primers utilized were designed by Primer 3 software and are shown in Table 2.1. Reaction was carried out in 20 μl volumes using SYBR Green PCR master mix (Applied Biosystems). Then PCR was started with 95℃, 10 minutes, followed by 40 cycles of denaturation at

94℃ for 10 seconds, annealing at 58℃ for 20 seconds and elongation at 72℃ for 30 seconds. The relative expression of each gene was calculated as the ratio to 60S ribosomal protein L32 (RPL32).

Cell culture and conditioned medium (CM)

The canine OSA cell lines (HMPOS and CHOS) were cultured as described in Chapter 1. CM from canine OSA cell lines was collected using a modified method previously reported by Costa-Rodrigues et al., (2010). Briefly, CM was obtained from the cells at 80-90% confluence, and culture supernatant collected was subsequently centrifuged at 3000 rpm for 10 minutes. Supernatant was stored at -80℃ until further use.

Co-culture with conditioned medium of OSA cell lines

To evaluate the osteoclastogenic potential of CM derived from HMPOS and CHOS cell lines on canine BMCs, the OC formation activity by the CM was investigated by using *in vitro* OC formation assay with slight modifications

(Costa-Rodrigues et al., 2010; Lau et al., 2007; Miyamoto et al., 2002). BMCs solutions were washed, followed by the same process as described in OCs differentiation method. Once differentiated cells were detached, they were cultured with 10 ng/ml M-CSF at the concentration of 1.5 x 10^5 cells/well in 48-well plates, and divided into following groups; two controls (absence or presence of 30 ng/ml RANKL), and HMPOS-CM or CHOS-CM with or without 30 ng/ml RANKL.

To determine the dose dependent manner in OC formation, the effect of variety of RANKL doses (10, 20, or 30 ng/ml) was investigated. At the end of co-culture, the cells were subjected to TRAP staining for OC identification. TRAP-positive cells with 3 or more nuclei were counted.

Statistical analysis

The mean and SD of the mRNA expression and number of OCs were calculated. The mRNA expression was compared among OCs differentiation state using the Tukey-Krammer multiple comparisons tests. The statistical comparison of OCs was made by using Student's *t*-test. $P<0.05$ was designed as statistically significant.

Results

Canine OCs differentiated from canine BMCs *in vitro*

Fig.3.1.2 shows OC-like multinucleated cells differentiated from canine BMCs. When BMCs were stimulated with M-CSF and with or without RANKL, OC-like multinucleated cells (OC-like cells) appeared after 2 days and their number reached a maximum on day 4. However, these cells formed under the absence of RANKL did not show any OC characteristics, while BMCs cultured under the presence of RANKL exhibited typical characteristics of OCs, including TRAP positivity, actin ring formation and pit formation activity on dentine slices, thereby meeting the major criteria for classification as OCs. TRAP staining revealed strong staining at the central of cells (Fig.3.1.2 A). Rhodamine staining demonstrated strong marginal “actin ring” at the periphery of multinucleated cells (Fig.3.1.2 B). Additionally, these cells showed lacunar resorption pit on dentin slices (Fig.3.1.2 C).

Canine OC marker expressions

Fig.3.1.3 shows the mRNA expression of OC-specific markers. There was a significant increase in all specific markers on 4th day after starting M-CSF and RANKL stimulation. The relative increase in the expression levels of the OC-specific markers 4 days after RANKL stimulation was 11.6 times for NFATc1, 73.8 times for Calcitonin-R, 14.3 times for RANK, and 29 times for MMP9, respectively.

Differentiation of OC-like multinucleated cells with CM

Fig.3.1.4 shows OCs induction from BMCs co-cultured with either HMPOS-CM or CHOS-CM. Although OC-like multinucleated cells were formed under the presence of M-CSF and 30% CM, they were all TRAP-negative, and addition of RANKL induced formation of TRAP-positive cells (Fig. 3.1.4 A, B). Furthermore, the number of TRAP-positive OCs was significantly higher with CHOS-CM by 1.2 fold, while significantly lower with HMPOS-CM by 2 fold when compared with the control. In addition, CHOS-CM differentiated 3 times more TRAP-positive cells than HMPOS-CM (Fig. 3.1.4 C).

Fig.3.1.5 shows OCs by addition of various doses of RANKL. The number of OCs formed in HMPOS-CM and CHOS-CM increased as the RANKL dose was increased from 10 ng/ml to 30 ng/ml. Moreover, the number of OCs formed with CHOS-CM was significantly higher than with HMPOS-CM at each RANKL dose as follows; 2.5 times for 10 ng/ ml RANKL (p=0.00013), 2.2 times for 20 ng/ml RANKL (p=0.0003), and 136.7 times for 30 ng/ml RANKL (p=0.0000038), respectively (Fig.3.1.5 C).

Discussion

In this section, it was demonstrated that multinucleated cells were differentiated from canine BMCs *in vitro* by adding M-CSF and RANKL. These multinucleated cells showed typical OC characteristics with positive in TRAP staining, rhodamine phalloidin staining, pit formation assay, and expression of OC-specific markers. When RANKL was absent in the culture medium, multinucleated cells were formed but they did not show OCs characteristics. It was confirmed that presence of both M-CSF and RANKL was indispensable to induce canine OCs differentiation, similar to the previous report (Boyle et al., 2003).

Several canine OC differentiation methods have been reported. Bird et al. reported canine OC differentiation from BMCs *in vitro*, and differentiated cells exhibited morphological features of OCs as determined by electron microscopy. However, the number of OCs obtained was too small to be subjected to the biochemical analysis, and they failed to develop resorption pits on dentine slices (Bird et al., 1992). Mee et al. also reported canine OCs induced from BMCs under the presence of

1α,25-dihydroxyvitamin D_3. Although the cells were positive for Calcitonin-R as determined by autoradiography, their bone-resorbing activity was poor, and the expression of OC-specific markers was not clarified (Mee et al., 1995).

From our best knowledge, this was the first report on the successful induction of canine OCs with OC-specific marker expression and bone-resorbing activity *in vitro*. This OC differentiation method is thought to be useful for the future investigation on canine OC-related disorders.

Furthermore, osteoclastogenic potential of CM derived from HMPOS and CHOS cell lines on canine BMCs was evaluated in the absence of physical cell interaction. Co-culture with canine BMCs and CM from either HMPOS or CHOS alone was unable to induce TRAP-positive cells. However, addition of RANKL to CM induced formation of TRAP-positive OCs. In all tested conditions, TRAP positivity was associated with the presence of 30 ng/ml RANKL, which concentration was lower than used in the OC differentiation method. This may suggest the concentration of RANKL in CM from both cell lines was not enough to promote osteoclastogenesis. According to the increase in RANKL added to the culture medium, osteclastogenesis was accelerated.

The number of TRAP-positive cells was less when HMPOS-CM was added with RANKL, compared to the number of TRAP-positive cells observed in CHOS-CM with RANKL. These *in vitro* experiments agreed the phenomenon observed in Chapter 1; the tissues in HMPOS-xenograft mice did not show OCs at the interface of the tumor and bone, while those in CHOS-xenograft mice showed increase in OCs at the interface. Thus HMPOS may have suppressive effect on osteoclastogenesis *in vivo*, while CHOS supported osteoclastogenesis with higher RANKL production.

One study reported that twelve cloned cells established from human OSA cell line were co-clutured with human monocytes, among which three cloned cells showed an ability of inducing OCs. These three cloned cells showed expression of TNF-α converting enzyme (TACE) which was known to be associated with cleavage of RANKL from OSA cells to be released to CM (Miyamoto et al., 2002). It is also known that membranous RANKL produced by osteoblasts or stroma cells plays a major role in OCs differentiation via cell-to-cell interaction with OC-progenitors (Suda et al., 1992). In agreement to the previous report, although soluble RANKL produced by CHOS cells was insufficient to induce OC differentiation *in vitro*, direct interaction between tumor

cells and OC-progenitors may be essential in the xenograft mouse model used in this study. RANKL derived from canine OSA cells may have additive effect on osteoclastogenesis *in vivo*, leading to tumor-induced osteolysis. Thus, to clarify the potential of anti-RANKL antibody on canine OSA, the efficacy should be evaluated on the CHOS-xenograft mouse model.

Section 2: Effect of anti-RANKL antibody on the growth of OSA in a xenograft mouse model

Materials and Methods

Cell culture

CHOS was used in this study due to its high RANKL expression. The cell was cultured with the same condition as previously described in Chapter 1.

Administration of anti-mouse RANKL neutralizing monoclonal antibody

Anti-mouse RANKL neutralizing monoclonal antibody (OYC1) was kindly provided by Oriental Yeast Co., Ltd, Tokyo, Japan. CHOS ($1x10^5$ cells/head) were transplanted into the tibia of 5-week-old male BALB/c nude mice (Japan SLC, Ltd.) as previously described in Chapter 1. Five mice were enrolled in both the control and treatment groups. In the previous report, a single injection of 5 mg/kg OYC1 subcutaneously was sufficient to increase bone mineral density (BMD) from day 2 to

day 28 (Furuya et al., 2011). Thus, saline (control group) or OYC1 at the dose of 5 mg/kg (treatment group) was subcutaneously injected once on the 2nd week, then mice were sarcrificed at the 3rd and 5th week after the transplantation.

μ-CT

μ-CT analysis was performed for the tibia of xenografted mice similarly to the method described in Chapter 1. Bone mineral content (BMC) and density (BMD) were also calculated from the μ-CT data.

Histopathology

Bone lesions of the tibia were fixed with 10% buffered formalin and decalcified with 10% EDTA solution at 4 ºC for 2 to 3 weeks as described in Chapter 1. Then they were paraffin-embedded, sectioned longitudinally at 3 μm thickness and stained with HE and TRAP. Tumor areas of the lesions were measured by using Image J (NIH) and the number of OCs at the interface of the tumor and bone were counted and defined as the number of OCs under the area.

Immunocyto / histochemistry for Ki67

ICC and IHC were performed using the same methods as described in Chapter 1. ICC was performed on CHOS cells under the absence or presence of OYC1. The dose of OYC1 added to CM was calculated as a similar proportion to that injected to CHOS-xenografted mice. CHOS cells were seeded at a density of $5x10^3$ cells/well onto Lab Ⅱ 8-well chamber slides (Thermo Fisher Scientific Inc.) and incubated with absence or presence of OYC1 at 37℃for 24 hours. After aspiration of culture medium, cells were fixed with 4% paraformaldehyde / PBS at room temperature for 30 minutes with gentle shaking. After washing with PBS for 3 times, cells were subjected to 3 N HCL at room temperature for 20 minutes, followed by the same procedure of IHC described in Chapter 1. Mouse anti-mouse Ki67 antibody (DAKO) was used in ICC and IHC at dilutions of 1:500 and 1:100, respectively.

Evaluation of proliferation index (PI)

Random 5 high-power fields were selected and 1,000 OSA cells in both cultured cells and tissues developed in CHOS-xenografted mice were counted. The

percentage of Ki-67-positive cells was calculated as proliferation index (PI).

Statistical analysis

The mean and SD of BMD, BMC, the tumor area, the number of OCs and Ki-67 positive cells were calculated. The comparison between the control and treatment groups was statistically analyzed by Student's *t*-test. $P<0.05$ was considered statistically significant.

Results

Effect of anti-RANKL antibody on skeletal lesions of xenografted mice

Fig.3.2.1 shows three-dimensional μ-CT images of mice of each group. Osteolysis was clearly observed in all the mice of the control group after 3rd week, and at 5th week, the lesion considerably progressed (Fig.3.2.1 A). In contrast, the osteolytic lesions were only observed in one mouse in the treatment group, in which osteolysis was much smaller than those in control mice. These images also showed the thickening of methaphysis of the tibia distal to the lesion. Sagittal sections of the tibia showed the loss of continuity of the cortical bone in control animals, while the continuity of the cortical bone was well preserved in the treatment group (Fig. 3.2.1 B, C).

Fig.3.2.2 shows the change in BMC and BMD of the bone cortex. BMC of the treated mice was significantly higher than that of the control at either 3rd (p=0.011) or 5th (p=0.000012) week of transplantation. BMD was also significantly higher in the treatment group compared to the control group at 5th week of the transplantation (p=0.027).

Histopathology

Fig.3.2.3 shows histopathological findings of the tibia of CHOS-xenografted mice. On the lesion of the control group, a number of TRAP-positive OCs were observed at the interface of the tumor and bone (Fig.3.2.3 B). On the other hand, few OCs were observed in the tissues of the treatment group.

Fig.3.2.4 shows tumor areas and number of OCs at the interface of the tumor and bone on the tumor tissues of each group. Individual histopathological analysis showed that 20% of mice in the treatment group formed a primary tumor, while 100% of mice enrolled in the control group developed the primary tumor. Tumor areas of the control group were significantly larger than those of the treatment group at 3rd and 5th week of transplantation (p=0.0020 and p=0.0025, respectively) (Fig.3.2.4 A). Number of OCs in the control group was significantly higher than those of the treatment group at 3rd week (p=0.000089) and 5th week (p=0.00059) (Fig.3.2.4 B).

Immunocyto / histochemistry for Ki-67

Fig.3.2.5 shows ICC findings for Ki-67. Ki-67 expression was localized in the nuclei of OSA cells, and there was no significant difference in Ki-67-positive cells between the control and treatment groups *in vitro* (p=0.1454). In contrast, immunohistochemical analysis for bone tissues from CHOS-transplanted mice showed a significant reduction in Ki-67-positive cells in the treatment group compared to the control at 3rd week (p= 0.00031) and 5th week (p= 0.027) of transplantation (Fig.3.2.6).

Discussion

Therapeutic potential by inhibiting the RANK/RANKL pathway in the treatment of OSA has been confirmed by the recent studies, which demonstrated that administration of OPG cDNA (Lamoureux et al., 2007), RANK-Fc protein or cDNA (Akiyama et al., 2010, Lamoureux et al., 2008), and siRNA targeting RANKL (Rousseau et al., 2011) suppressed osteolytic lesions associated with OSA.

The control mice transplanted with CHOS cells into the tibia exhibited progressive osteolysis with a number of OCs at the interface between the tumor and bone tissues, where strong RANKL expression was observed. Administration of OYC1 to CHOS-xenografted mice reduced the number of OCs at the lesion of the tibia, and suppressed tumor-induced osteolysis, resulting in an increase in BMC and BMD. This result was similar to the report, in which the change was observed in BMD of normal mice with a single injection of 5 mg/kg (Furuya et al., 2011). They also found increase in BMD of the trabecular bone especially in the distal metaphysis. However trabecular

BMC and BMD were unable to evaluate due to the limitation of μCT system used in this study.

When the tumor volume was calculated by measuring the largest and smallest perpendicular tibia diameters, there was a decreasing tendency of the tumor volume, while no statistical difference was obtained. Furthermore, only 20% of mice formed the primary tumor in the treatment group, while all mice in the control group developed the primary tumor on histopathological analysis. Though, the tumor growth was not evident enough to show detectable volume change, when the tumor area was measured on histopathological sections, the area was markedly reduced in the treatment group. Lamoureux et al. also reported that OPG gene transfer was effective in human OSA tumor-inoculated mouse model to prevented osteolysis at the transplanted lesions, and only 30% of mice showed development of the primary tumor in the treatment group (Lamoureux et al., 2007).

In addition, number of OCs was significantly suppressed in the treatment group. This result was supported by Furuya et al., in which the effect of OYC1 on the

bone started to appear from the 2nd day and maintained OCs suppression until 28th day after injection.

Since the reduction in the tumor area in the antibody-treated mice might be due to the direct tumoricidal effect of the antibody, I examined the effect of OYC1 on the growth of CHOS cells *in vitro*. Treatment with OYC1 did not affect the ratio of the Ki-67-positive cells *in vitro*, though Ki-67-positive tumor cells were dramatically reduced in the tissues developed in the treated mice *in vivo*. These results suggest that OYC1 did not directly inhibit tumor cell growth *in vitro*, but suppressed the release of tumor growth factors from OCs or bone matrix essential for resorption by OCs, leading to suppression of tumor growth. Bone is known to give a soil for tumor colonization and proliferation (Mundy, 2002), therefore, anti-RANKL antibody may inhibit the formation of the tumor niche by suppressing bone resorption.

These data support the hypothesis of the vicious cycle induced by OSA (Akiyama et al., 2008; Mundy, 2002). RANKL expression on canine OSA may relate to tumor-induced bone osteolysis by inducing OC differentiation, which in turn causes

tumor cell proliferation. Anti-RANKL antibody is therefore a promising therapeutic agent for OSA treatment.

Table.3.1 Sequence of primers used for the real-time PCR

Gene	Forward primer (5' - 3')	Reverse primer (5' – 3')	Product size (bp)
NFATc1	CACAGGCAAGACTGTCTCCA	TCCTCCCAATGTCTGTCTCC	176
Calcitonin-R	TGAGCAAAATGAGGGAAACC	CACTGACGCTTCACAGTGGT	247
RANK	CCCTGGACCAACTGTAGCAT	ACCCAGTGCCACAAATTAGC	239
MMP9	GAGTTTCGACGTGAAGACGCAGAC	CAAAGGTCACGTAGCCCACTT CGT	200
RPL32	TGGTTACAGGAGCAACAAGAA	GCACATCAGCAGCACTTCA	100

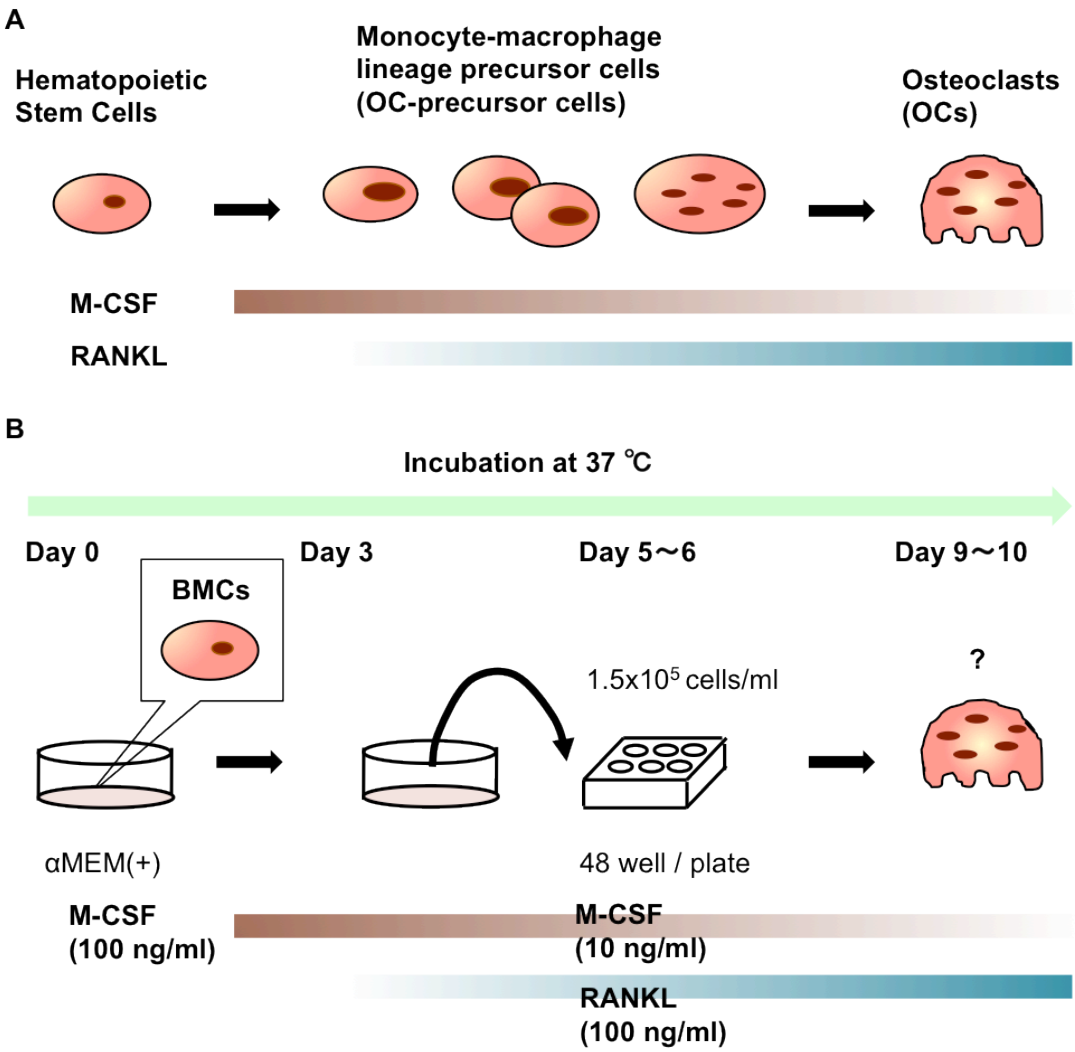

Fig. 3.1.1 The schematic diagram showing the process of canine osteoclastogenesis from canine BMCs *in vitro*. (A) OCs are hematopoietic stem-derived cells and two essential molecules, M-CSF and RANKL, are indispensable for *in vitro* osteoclastogenesis. M-CSF mainly effects on the earlier stage to increase survival of OC precursor cells, whereas RANKL effects on the later stage of osteoclastogenesis and induces OCs differentiation and maintains the survival of mature OCs. (B) Canine BMCs were obtained and incubated for 5 to 6 days with medium containing 100 ng/ml M-CSF. The cells were adjusted to 1.5 x 10^5 cells/ml, seeded to a 48 well/plate with M-CSF (10 ng/ml) and RANKL (100 ng/ml), and incubated for another 4 days, then they were utilized for subsequent OC analysis.

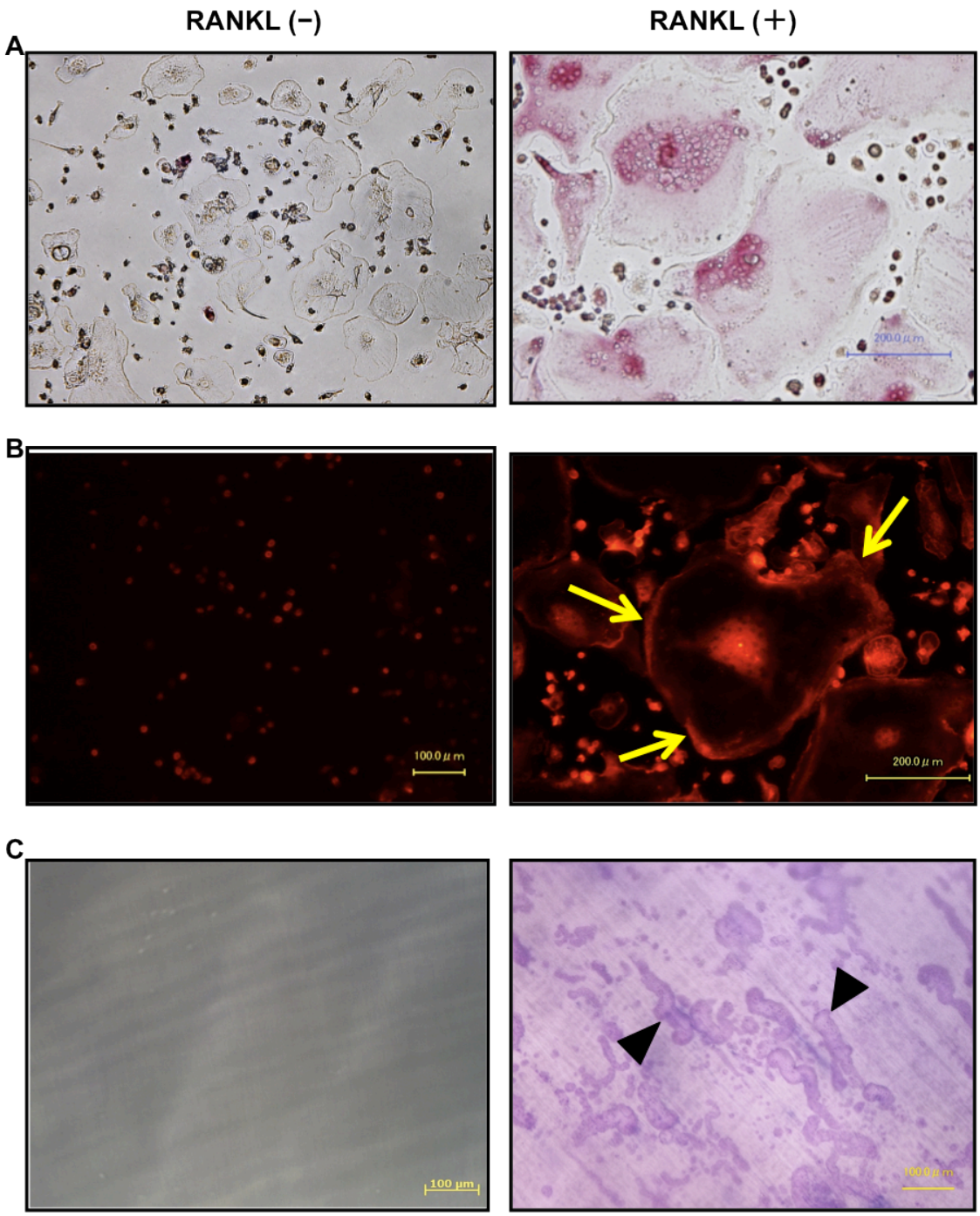

Fig.3.1.2 OC-like cells differentiated from canine BMCs. Under the absence of RANKL (left columns), OC-like cells did not show the characteristics of OCs. Under the presence of RANKL (right columns), (A) TRAP staining showed the presence of activated OCs. (B) An “actin ring” was present at the periphery of multinucleated cells (arrows); rhodamine phalloidin staining. (C) The formation of lacunar resorption pit on dentin slices (arrowheads).

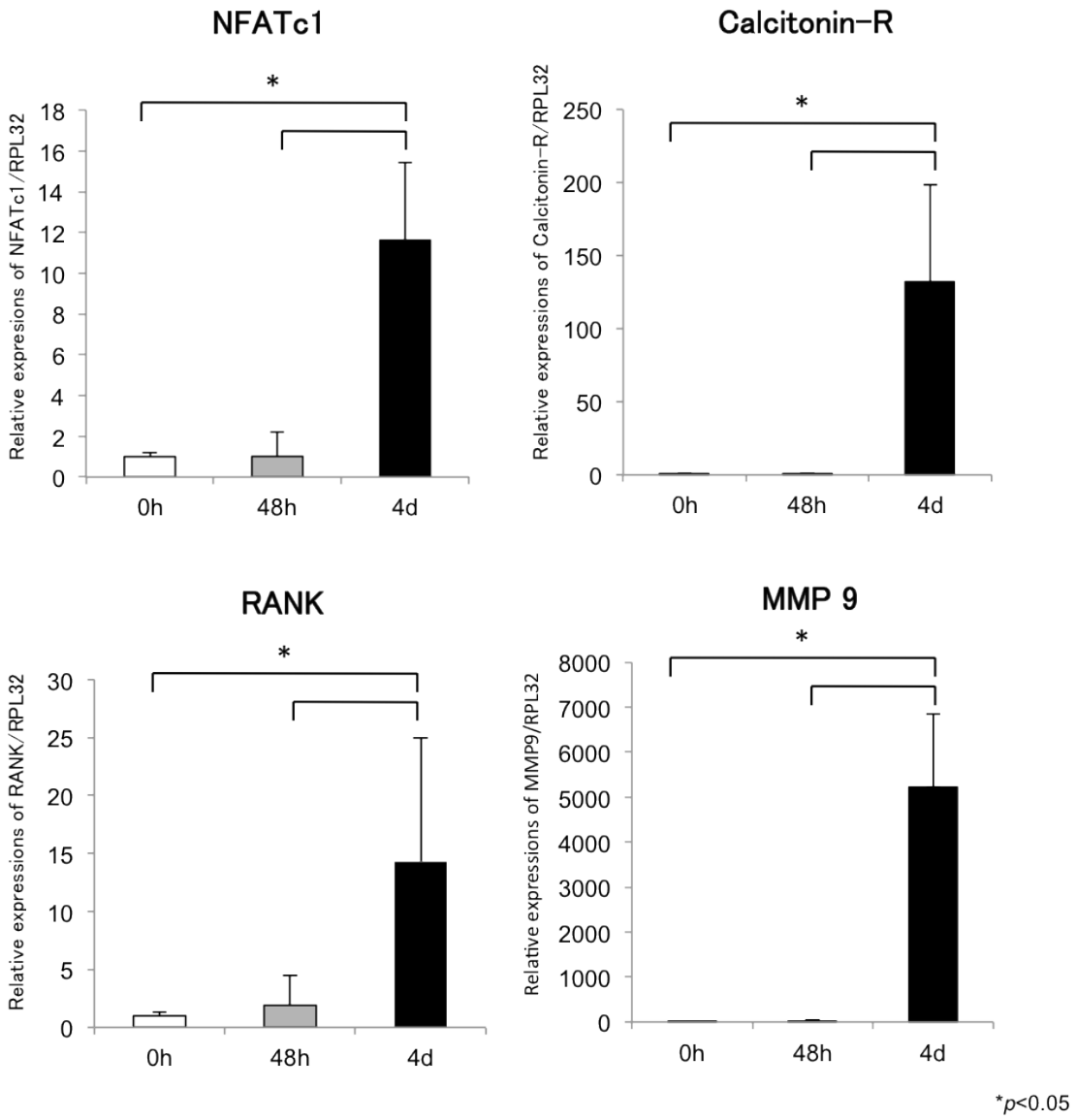

Fig.3.1.3 mRNA expressions of specific canine OC markers (NFATc1, Calcitonin-R, RANK and MMP9). There were significant increases in all these markers in 4th day after starting M-CSF (10 ng/ml) and RANKL (100 ng/ml) stimulation. * represented significant difference (p<0.05) compared to 0h; vertical bars represents SD.

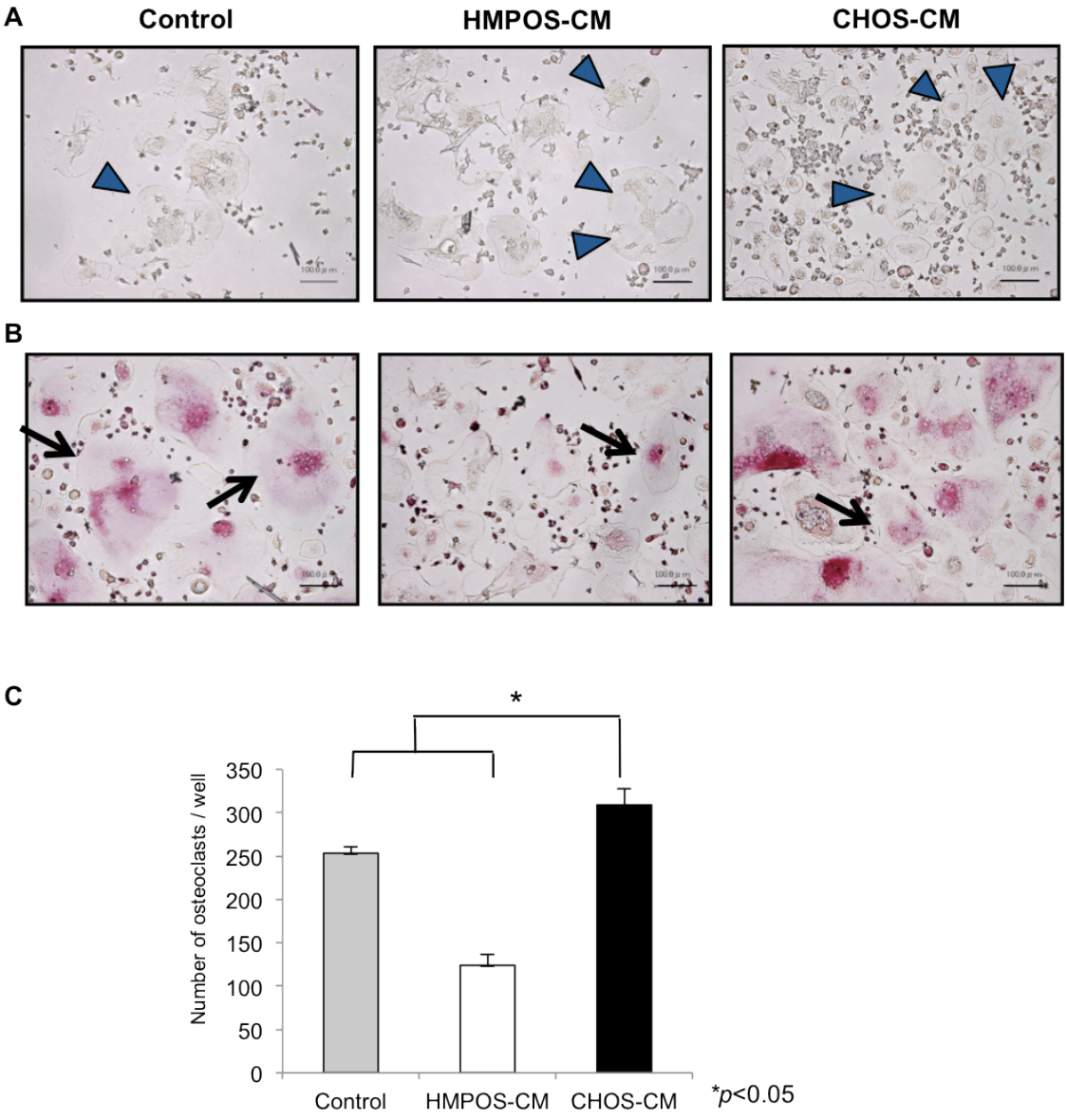

Fig.3.1.4 OCs differentiation from BMCs co-cultured with either HMPOS-CM or CHOS-CM under the absence or presence of RANKL (30 ng/ml). (A) Under the absence of RANKL, multinucleated cells were TRAP-negative (arrowheads). (B) Addition of RANKL induced TRAP-positive OCs in all groups (arrows). (C) Total number of TRAP-positive OCs under the presence of RANKL were counted. *Significant difference (p<0.05); vertical bars represent SD.

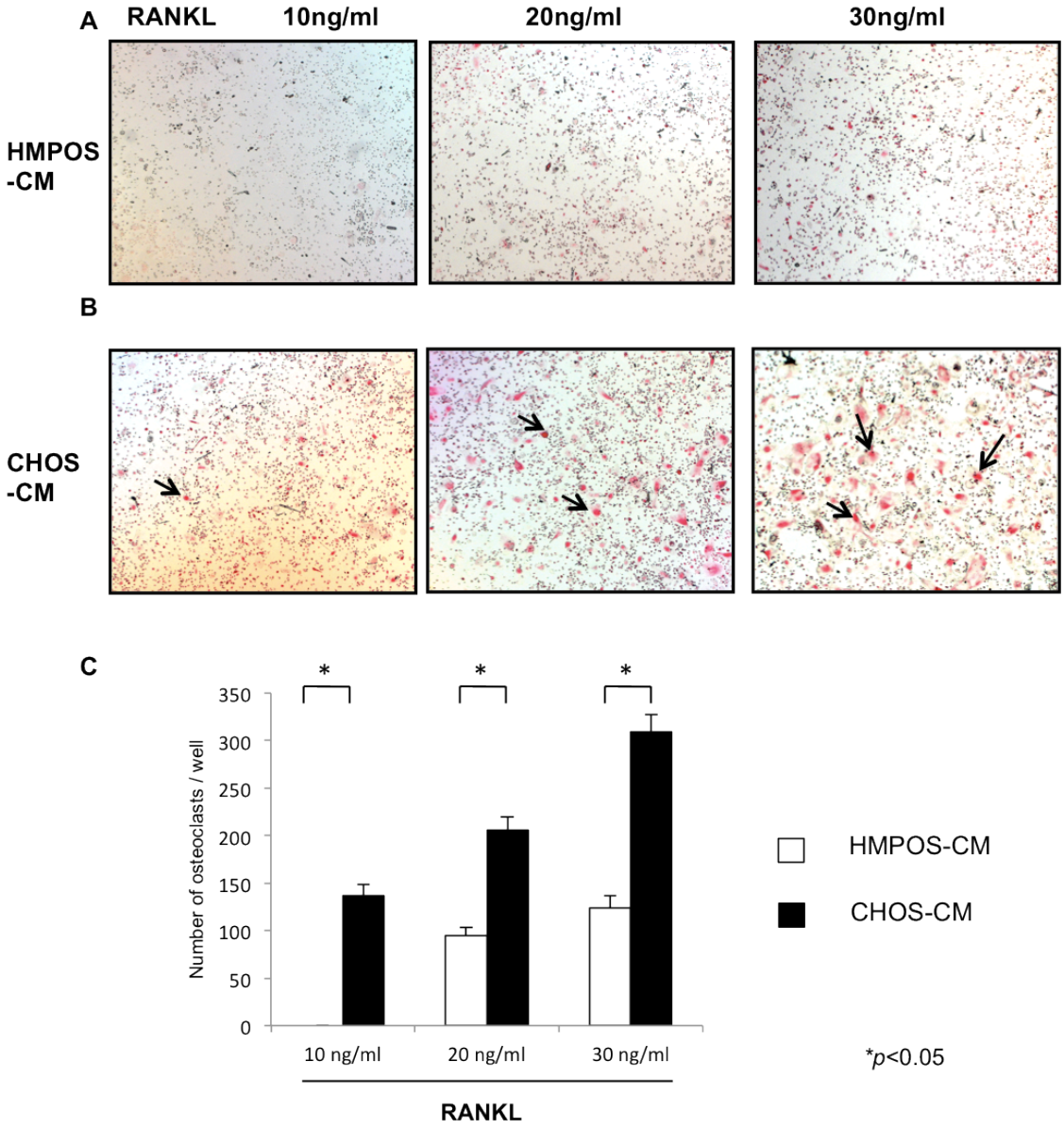

Fig.3.1.5 Osteoclastogenesis by RANKL of various doses. BMCs were incubated with M-CSF, CM from HMPOS (A) or CHOS (B), and the various doses of RANKL. Many OCs were seen by CHOS-CM (arrows). (C) The number of OCs induced with CHOS-CM was significantly higher at each RANKL dose. *Significant difference (p<0.05); vertical bars represents SD.

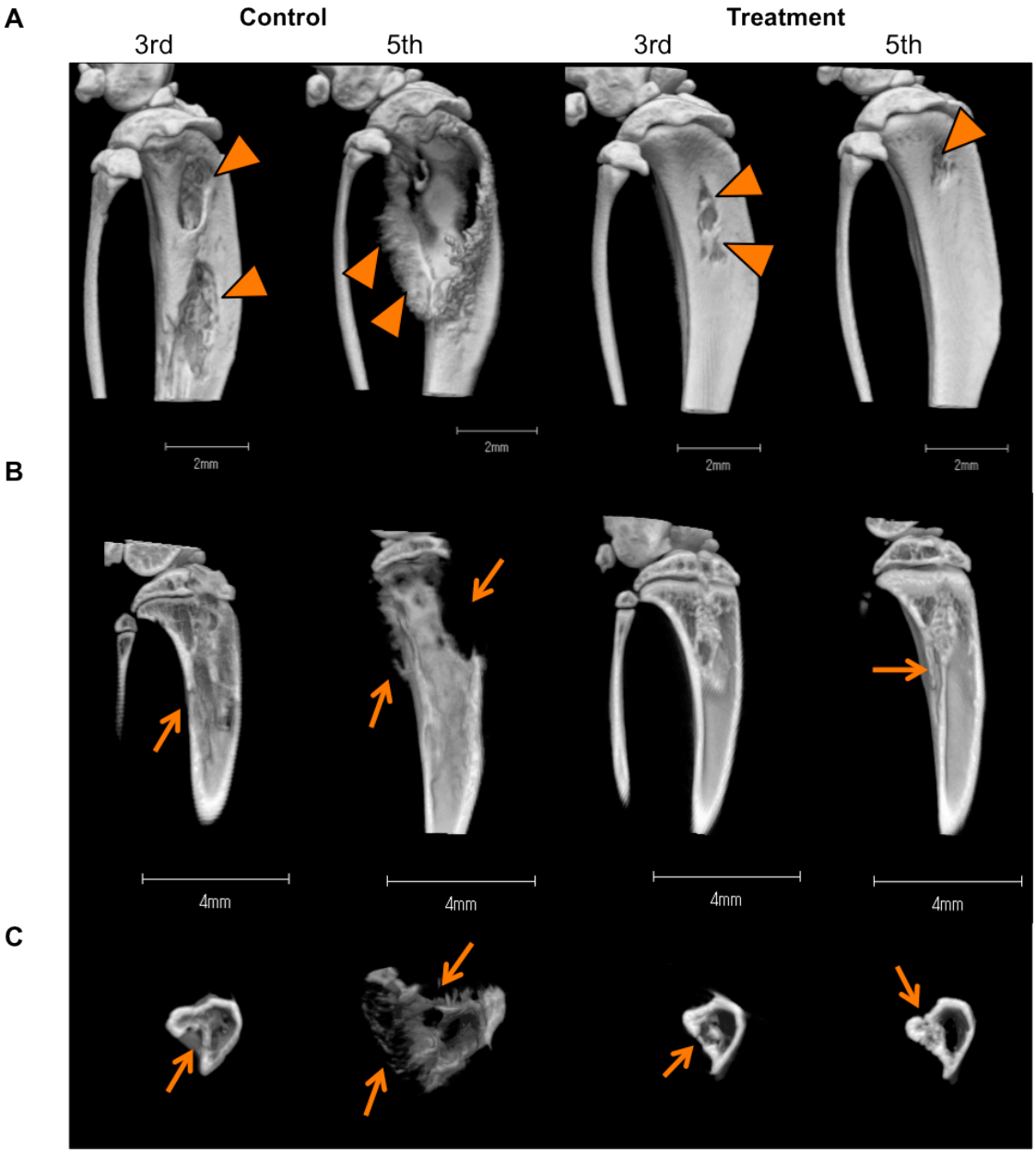

Fig. 3.2.1 Three-dimensional μ-CT images of the tibia showing bone resorption at 3rd and 5th week in mice of the control and treatment groups. (A) Clear osteolysis (arrowheads) was observed in all mice in the control group at 3rd week, and became severer at 5th week, while osteolysis was much smaller in the treatment group. (B) (C) Sagittal and cross sections of the tibia in both groups. Osteolysis caused loss of continuity of the cortical bone in mice of the control groups. On the contrary, the tibia of the treated group showed much less osteolysis (arrows).

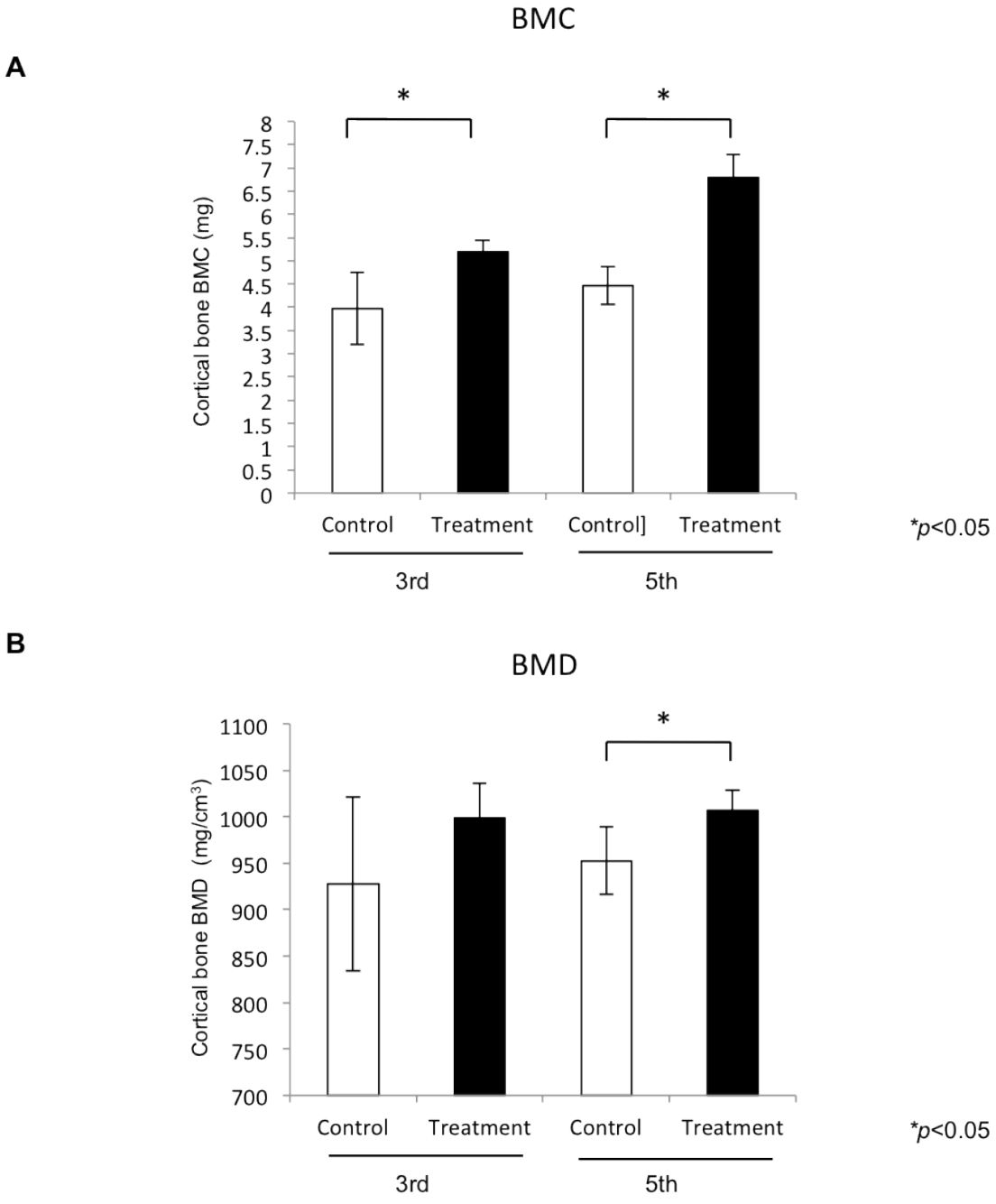

Fig. 3.2.2 BMC and BMD of the cortical bone around the lesion. (A) BMC of the treatment group at 3rd (p=0.011) and 5th (p=0.00012) week was significantly higher than that of the control group. (B) BMD was significantly higher at 5th week in the treatment group than the control group (p=0.027). * represented significant difference (p<0.05) compared to control; vertical bars represents SD.

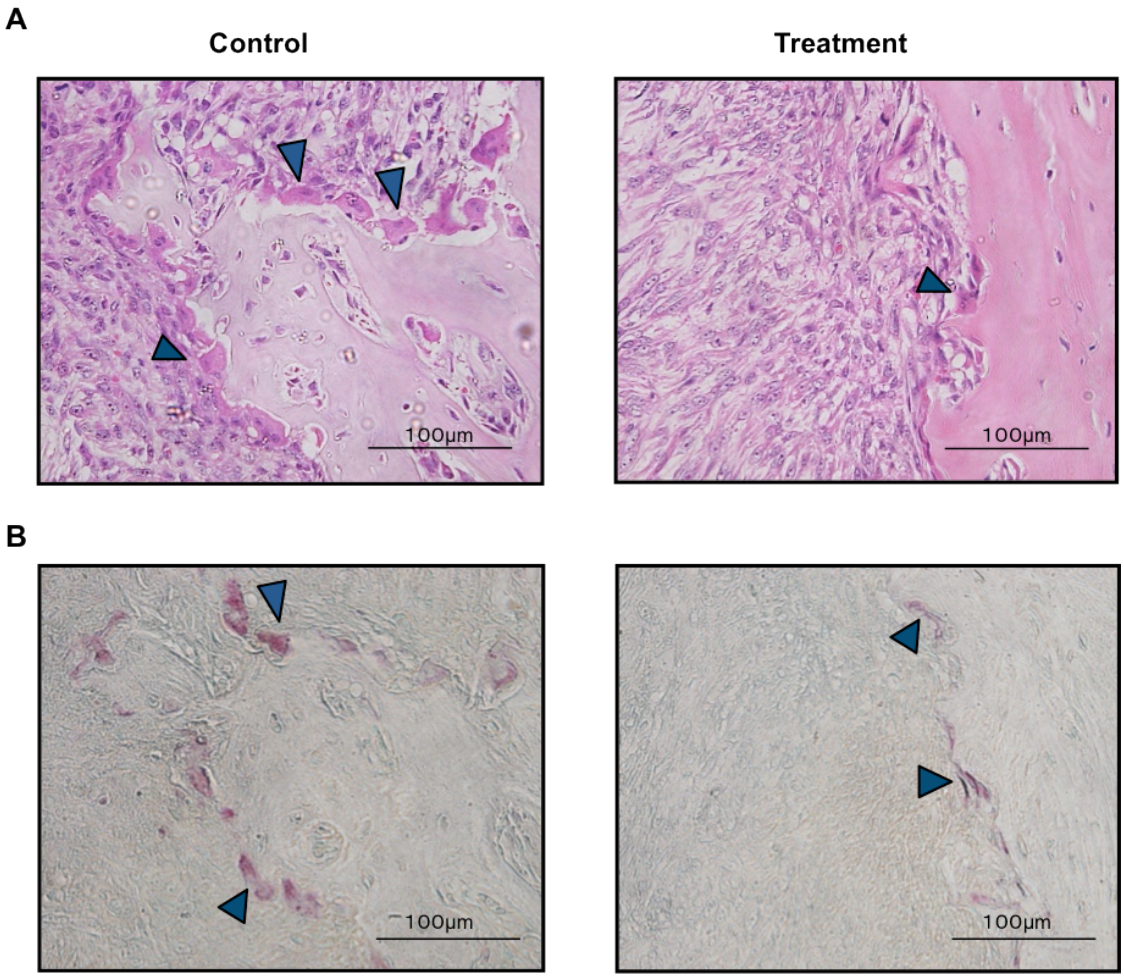

Fig. 3.2.3 Histopathological findings of the lesion in both treated and control mice.

HE staining (A) and TRAP staining (B) . (A) Numerous multinucleated cells were observed at the interface of the tumor and bone cortex in the control mice, while fewer cells were observed in the treated mice. (B) All the multinucleated cells were TRAP-positive OCs.

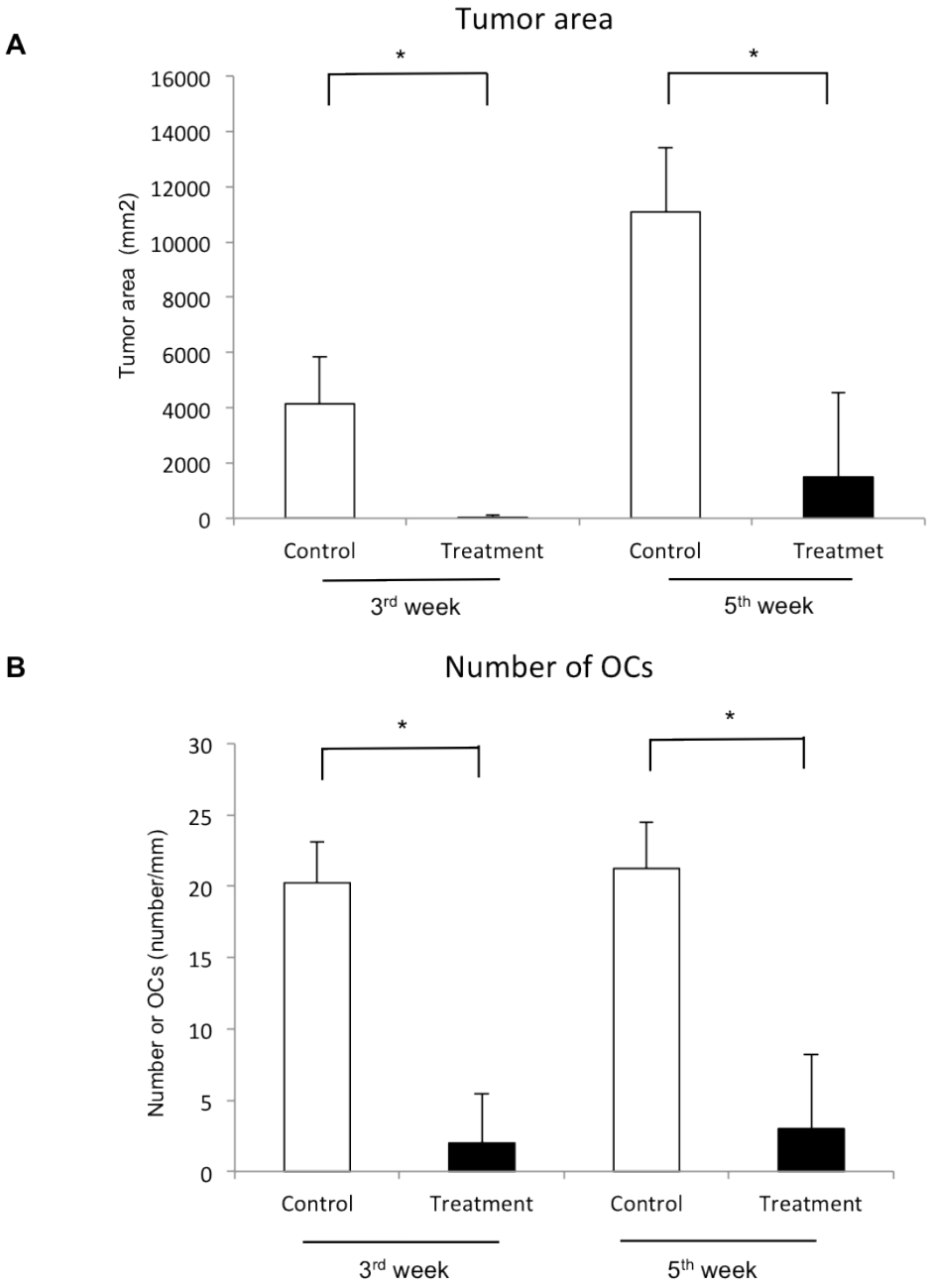

Fig. 3.2.4 Number of OCs at the interface of the tumor and bone , and tumor area in the tissues of each group. (A) Tumor area showed significant difference between the groups. (B) Number of TRAP-positive OCs at the interface of the tumor and bone. There was a significant difference between the control and treatment groups at 3rd and 5th week of transplantation. *Significant difference (p<0.05); verticle bars, SD.

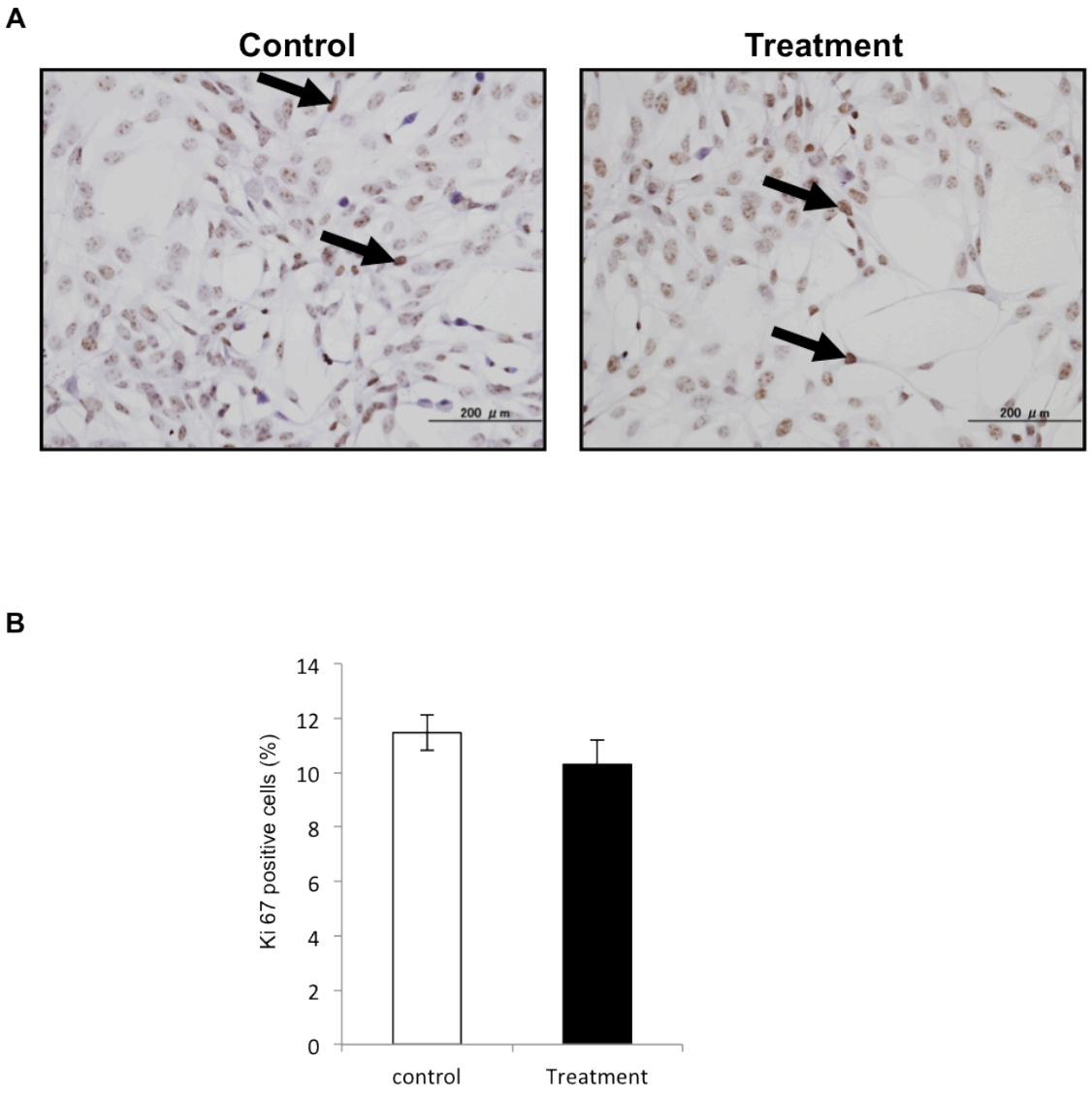

Fig. 3.2.5 Ki-67 expression on CHOS cell line. (A) Immunocytochemistry for Ki-67-positive cells (arrows). Ki-67 expression was localized in the nucleus of CHOS cells. (B) There was no significant difference in Ki67-positive cells between the control and treatment groups (p=0.1454).

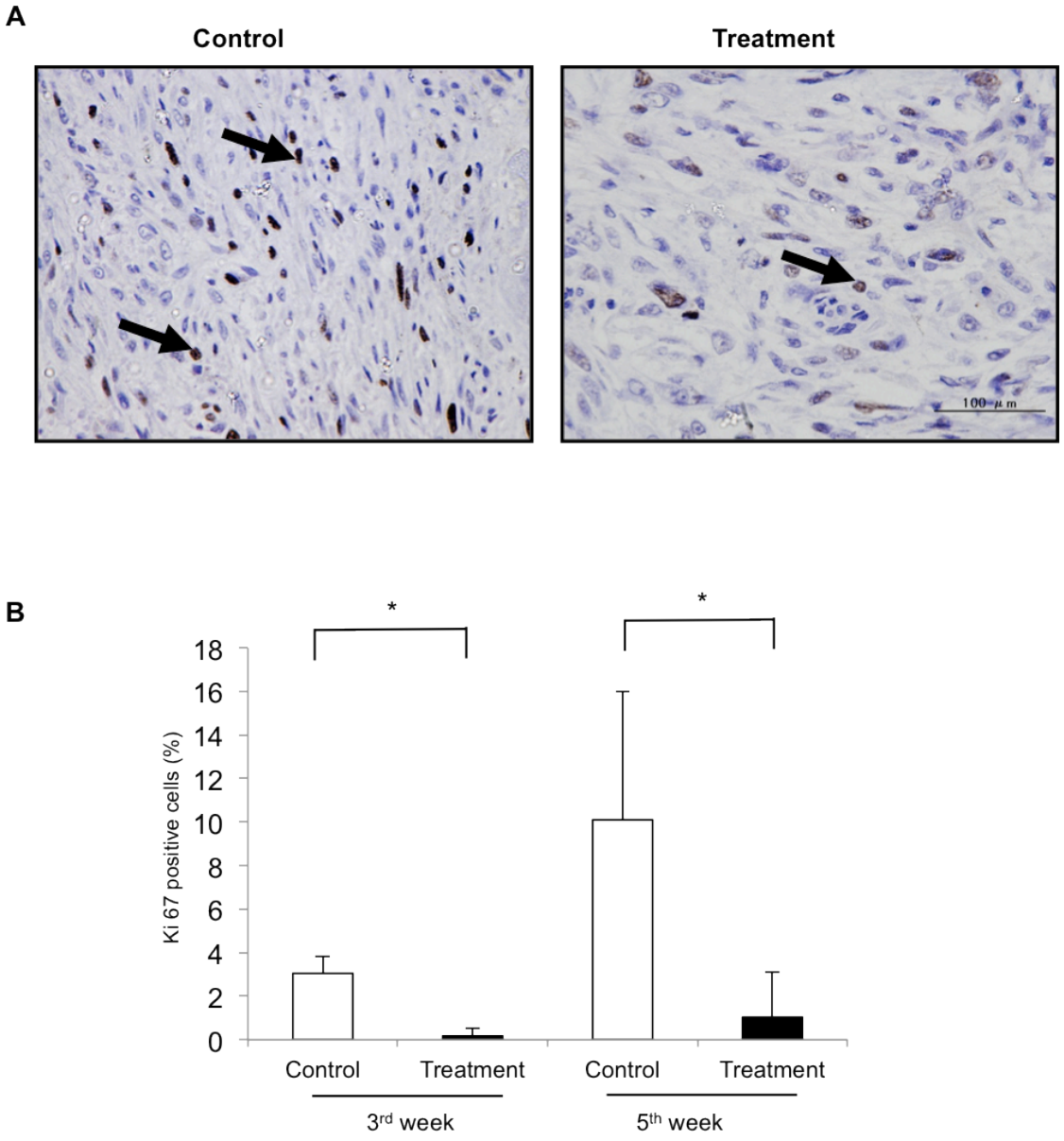

Fig. 3.2.6 Ki-67 expression on tissues of CHOS-xenografted mice.

(A) Immunohistochemistry for Ki-67-positive cells (arrows). (B) Ki-67 positive cells were significantly decreased on the tissues of the treatment group from 3rd and 5th week. *Significant difference (p<0.05); vertical bars, SD.

Conclusion

In OSA, bone lesions often cause severe pain due to bone destruction and pathological fracture (Boulary et al., 1987). Tumor-induced osteolysis is considered to be associated with OC activity. OCs are derived from monocyte-macrophage lineage precursor cells, and their differentiation is strictly regulated by two essential cytokines, M-CSF and RANKL. RANKL, a member of TNF superfamily, is expressed on the surface of osteoblasts in response to various hormones and cytokines, and binds to its specific receptor RANK expressed on OC precursors. M-CSF regulates the survival and fusion of OC precursors at an early stage, while RANKL is essential for the subsequent differentiation and maturation.

RANK and RANKL are the crucial factors for OC-related biology and also known to be involved in the process of bone destruction in both primary and metastatic bone tumors. Tumor cells themselves are unable to resorb bone matrix directly, therefore tumor-mediated OC differentiation is required for bone resorption, which must take place before the tumor cells grow and invade into the bone microenvironment. It is also suggested that several tumor cells produce RANKL, which promotes osteoclastogenesis and releases the growth factor from bone matrix, resulting in tumor

proliferation. This vicious cycle is well explained for development of the primary and metastatic bone tumor.

The aim of this study was to clarify involvement of RANK-RANKL in pathophysiology of canine OSA, especially in the tumor growth and skeletal changes. In addition, since OC-targeted therapy has been drawn great attention as a novel therapy for the primary and metastatic bone tumors in human, the effect of anti-RANKL neutralizing antibody on the growth and bone lesions of canine OSA was investigated using a xenograft mouse model with canine OSA cell lines.

In Chapter 1, I initially investigated the expression of RANK and RANKL on tissues from canine OSA patients and 4 canine OSA cell lines (POS, HMPOS, OOS and CHOS) in section 1. Among 26 tissues of OSA patients, the expression of RANK and RANKL was found in 88.4% and 84.6% of the tissues, respectively. High RANKL expression was correlated with an increase in number of OCs in these patients. However, there was no significant correlation between RANK/RANKL expression and clinical variables including histological subtypes. Both RANK and RANKL were expressed on all 4 OSA cell lines. Relatively higher RANK protein expression was observed in POS,

while highest RANKL protein expression was observed in CHOS and lowest RANKL protein in HMPOS.

In section 2, a xenograft mouse model using HMPOS, low-RANKL-expressing cell line, and CHOS, high-RANKL-expressing cell line, was established to identify the relationship between RANK/RANKL expressions and tumor growth and skeletal changes *in vivo*. There was a significant difference in tumor volume, formation of metastatic nodules, and skeletal changes between HMPOS- and CHOS-xenografted mice. HMPOS-xenografted mice showed aggressive tumor growth with many metastatic nodules, while CHOS-xenografted mice did not show a significant change in tumor volume and no metastatic nodules throughout the observation period. Interestingly, histopathological findings revealed OCs induction at the interface of tumor and original bone in CHOS-xenografted mice, while low-RANKL expressing HMPOS did not induce OCs at the interface. Since RANKL is a crucial OC inducing factor, tumor-induced osteolysis found in CHOS-xenografted mice may be related to RANKL produced by CHOS, which promoted osteoclastogenesis *in vivo*.

In Chapter 2, I determined the function of RANK under RANKL stimulation using these two cell lines. Under RANKL stimulation, migration and invasion potential was significantly increased in HMPOS (high-RANK-expressing cell line), while in CHOS cell line (low-RANK-expressing cell line), no significant change in migration and significant suppression in invasion were observed. In HMPOS, phosphorylation of ERK1/2 and IκB was observed by RANKL stimulation, while in CHOS, phosphorylation of IκB was observed but dephosphorylation of ERK1/2 was also observed. Activation of p-38 and JNK was not evident in both cell lines. In addition, expression of MMP 2 and MMP 7 was observed in HMPOS after RANKL stimulation, suggesting these MMPs may play a key role to regulate motility and invasiveness of OSA cell lines.

These data support the hypothesis that RANKL expression on canine OSA may have correlation to metastatic potential such as migration and invasion of canine OSA through activation of MMPs via ERK and NFκB pathway.

In Chapter 3, I investigated whether RANKL released from OSA cells may have potential of osteoclastogenesis. Initially in section 1, the method of OC

differentiation from canine BMCs was established. BMCs were incubated with M-CSF and RANKL, and multinucleated cells obtained were subjected to the procedures of TRAP staining, actin ring formation and formation of lacunar resorption pit on dentine slice. The results showed that differentiation of OCs from canine BMCs was successfully demonstrated. In addition, real-time PCR demonstrated the expression of OC-specific markers (NFATc1, Calcitonin-R, RANK and MMP 9) in these differentiated OCs. To our best knowledge, this was the first report on successful differentiation of OCs from canine BMCs.

Furthermore, differentiation potential of tumor-derived RANKL in the conditioned medium (CM) from CHOS and HMPOS was examined. When canine BMCs were co-cultured with CM alone, active OCs were not differentiated, however addition of RANKL to CM, TRAP-positive OCs were induced. Moreover, the number of TRAP-positive cells was the least by HMPOS-CM while CHOS-CM formed significantly higher TRAP-positive cells. These results indicated that the concentration of RANKL in CM may not be sufficient to induce osteoclastogensis but RANKL derived from canine OSA cells line may have the function of induction of

osteoclastogenesis *in vivo*, which may lead to tumor-induced osteolysis.

In section 2 of Chapter 3, the suppressive effect of anti-RANKL neutralizing antibody on tumor growth and bone lesions was investigated in mice xenografted with CHOS, a highest RANKL-expressing cell line. Administration of anti-RANKL antibody to CHOS-xenografted mice significantly reduced the tumor volume compared to these in non-treated mice. In addition, osteolysis at the primary lesion was much suppressed in mice administered the antibody. In the tibia of treated mice, the number of OCs was also reduced and bone mineral content and density were significantly increased on μ-CT. The treatment with anti-RANKL antibody did not affect the ratio of Ki-67-positive cells *in vitro*, while Ki-67-positive cells were dramatically reduced in the treated mice *in vivo*. These results suggest that anti-RANKL antibody did not show the direct effect on tumor cells, but inhibited the release of tumor growth factor from OCs. According to these results, anti-RANKL neutralizing antibody may have suppressing effect on canine OSA development and protective effect on bone lesions through the suppression of OC differentiation, thus this antibody may be a promising therapeutic agent for OSA.

Acknowledgement

I would like to show my gratitude to all who made me possible to complete this thesis. I owe a deep debt of gratitude to my mentor, Prof. Nobuo Sasaki (Laboratory of Veterinary Surgery, Graduate School of Agricultural and Life Sciences, the University of Tokyo) for his continuous supervision, encouragement and support in all the time of the research.

Furthermore, I am sincerely grateful to Prof. Sakae Tanaka (Department of Orthopedic Surgery, Faculty of Medicine, the University of Tokyo) for his generosity in warm support and technical advice.

Moreover, I would like to give special thanks to Prof. Ryohei Nishimura (Laboratory of Veterinary Emergency Medicine, the University of Tokyo), Associate Prof. Manabu Mochizuki and Assistant Prof. Takayuki Nakagawa for their precious advice and support throughout this study. Furthermore, I greatly appreciate Mr. Jun Hirose, Mr. Hironari Masuda, Dr. Takumi Matsumoto and all members of Department of Orthopedic Surgery (Faculty of Medicine, the University of Tokyo) for their technical advice, support and kindness through this research. I am also deeply thankful to Dr. Jaroensong Tassanee for the technical assistance and helpful discussion, Mr. Muneki Honnami who worked hard together, for continuous moral support and encouragement, and all members of Laboratory of Veterinary Surgery, the University of Tokyo, especially members of cancer team for their cordial supports.

Unforgettably, I am deeply appreciative for Prof. Toshiyuki Yoneda (Department of Molecular and Cellular Biochemistry, Graduate School of Dentistry, Osaka University), Assistant Prof. Tomoki Nakashima (Department of Cell Signaling, Graduate School of Medical and Dental Science, Tokyo Medical and Dental University), and Assistant Prof. Yoshifumi Endo (Laboratory of Veterinary Clinical Oncology, Rakuno Gakuen University) for introducing me the great opportunity to investigate on osteoimmunology and giving me precise advice and warm encouragement.

Lastly, I would like to thank and dedicate this thesis to my parents and adorable family members, Jasmin, Pearl, Mint and Tanya who encouraged and supported me to accomplish the study at all times.

References

Akiyama, T., Choong, P.F., Dass, C.R., 2010, RANK-Fc inhibits malignancy via inhibiting ERK activation and evoking caspase-3-mediated anoikis in human osteosarcoma cells. Clin Exp Metastasis 27, 207-215.

Akiyama, T., Dass, C.R., Choong, P.F., 2008, Novel therapeutic strategy for osteosarcoma targeting osteoclast differentiation, bone-resorbing activity, and apoptosis pathway. Mol Cancer Ther 7, 3461-3469.

Akiyama, T., Dass, C.R., Shinoda, Y., Kawano, H., Tanaka, S., Choong, P.F., 2010, Systemic RANK-Fc protein therapy is efficacious against primary osteosarcoma growth in a murine model via activity against osteoclasts. J Pharm Pharmacol 62, 470-476.

Ando, K., Mori, K., Redini, F., Heymann, D., 2008, RANKL/RANK/OPG: key therapeutic target in bone oncology. Curr Drug Discov Technol 5, 263-268.

Avnet, S., Longhi, A., Salerno, M., Halleen, J.M., Perut, F., Granchi, D., Ferrari, S., Bertoni, F., Giunti, A., Baldini, N., 2008, Increased osteoclast activity is associated with aggressiveness of osteosarcoma. Int J oncol 33, 1231-1238.

Barger, A.M., Fan, T.M., de Lorimier, L.P., Sprandel, I.T., O'Dell-Anderson, K., 2007, Expression of receptor activator of nuclear factor kappa-B ligand (RANKL) in neoplasms of dogs and cats. J Vet Intern Med 21, 133-140.

Barroga, E.F., Kadosawa, T., Okumura, M., Fujinaga, T., 1999, Establishment and characterization of the growth and pulmonary metastasis of a highly lung metastasizing cell line from canine osteosarcoma in nude mice. J Vet Med Sci 61, 361-367.

Bergman, P.J., MacEwen, E.G., Kurzman, I.D., Henry, C.J., Hammer, A.S., Knapp, D.W., Hale, A., Kruth, S.A., Klein, M.K., Klausner, J., Norris, A.M., McCaw, D., Straw, R.C., Withrow, S.J., 1996, Amputation and carboplatin for treatment of dogs with osteosarcoma: 48 cases (1991 to 1993). J Vet Intern Med 10, 76-81.

Berlin, O., Samid, D., Donthineni-Rao, R., Akeson, W., Amiel, D., Woods, V.L., Jr., 1993, Development of a novel spontaneous metastasis model of human osteosarcoma transplanted orthotopically into bone of athymic mice. Cancer Res 53, 4890-4895.

Bird, M.C., Garside, D., Jones, H.B., 1992, Multinucleated giant cells in primary cultures derived from canine bone marrow--evidence for formation of putative osteoclasts. Cell Tissue Res 268, 17-30.

Bode, W., Fernandez-Catalan, C., Grams, F., Gomis-Ruth, F.X., Nagase, H., Tschesche, H., Maskos, K., 1999, Insights into MMP-TIMP interactions. Ann N Y Acad Sci 878, 73-91.

Boston, S.E., Ehrhart, N.P., Dernell, W.S., Lafferty, M., Withrow, S.J., 2006, Evaluation of survival time in dogs with stage III osteosarcoma that undergo treatment: 90 cases (1985-2004). J Am Vet Med Assoc 228, 1905-1908.

Bryden, A.A., Hoyland, J.A., Freemont, A.J., Clarke, N.W., George, N.J., 2002, Parathyroid hormone related peptide and receptor expression in paired primary prostate cancer and bone metastases. Br J Cancer 86, 322-325.

Boyle, W.J., Simonet, W.S., Lacey, D.L., 2003, Osteoclast differentiation and activation. Nature 423, 337-342.

Coleman, R.E., 1997, Skeletal complications of malignancy. Cancer 80, 1588-1594.

Costa-Rodrigues, J., Teixeira, C.A., Sampaio, P., Fernandes, M.H., 2010, Characterisation of the osteoclastogenic potential of human osteoblastic and fibroblastic conditioned media. J Biol Chem 109, 205-216.

Dickerson, M.E., Page, R.L., LaDue, T.A., Hauck, M.L., Thrall, D.E., Stebbins, M.E., Price, G.S., 2001, Retrospective analysis of axial skeleton osteosarcoma in 22 large-breed dogs. J Vet Intern Med 15, 120-124.

Ehrhart, N., Dernell, W.S., Hoffmann, W.E., Weigel, R.M., Powers, B.E., Withrow, S.J., 1998, Prognostic importance of alkaline phosphatase activity in serum from dogs with appendicular osteosarcoma: 75 cases (1990-1996). J Am Vet Med Assoc 213, 1002-1006.

Endo-Munoz, L., Cumming, A., Rickwood, D., Wilson, D., Cueva, C., Ng, C., Strutton, G., Cassady, A.I., Evdokiou, A., Sommerville, S., Dickinson,

I., Guminski, A., Saunders, N.A., 2010, Loss of Osteoclasts Contributes to Development of Osteosarcoma Pulmonary Metastases. Cancer Res 70, 7063-7072.

Forrest, L.J., Dodge, R.K., Page, R.L., Heidner, G.L., McEntee, M.C., Novotney, C.A., Thrall, D.E., 1992, Relationship between quantitative tumor scintigraphy and time to metastasis in dogs with osteosarcoma. J Nucl Med 33, 1542-1547.

Furuya, Y., Mori, K., Ninomiya, T., Tomimori, Y., Tanaka, S., Takahashi, N., Udagawa, N., Uchida, K., Yasuda, H., 2011, Increased bone mass in mice after single injection of anti-receptor activator of nuclear factor-kappaB ligand-neutralizing antibody: evidence for bone anabolic effect of parathyroid hormone in mice with few osteoclasts. J Biol Chem 286, 37023-37031.

Garzotto, C.K., Berg, J., Hoffmann, W.E., Rand, W.M., 2000, Prognostic significance of serum alkaline phosphatase activity in canine appendicular osteosarcoma. J Vet Intern Med 14, 587-592.

Hammer, A.S., Weeren, F.R., Weisbrode, S.E., Padgett, S.L., 1995, Prognostic factors in dogs with osteosarcomas of the flat or irregular bones. J Am Anim Hosp Assoc 31, 321-326.

Heyman, S.J., Diefenderfer, D.L., Goldschmidt, M.H., Newton, C.D., 1992, Canine axial skeletal osteosarcoma. A retrospective study of 116 cases (1986 to 1989). Vet surg 21, 304-310.

Hillers, K.R., Dernell, W.S., Lafferty, M.H., Withrow, S.J., Lana, S.E., 2005, Incidence and prognostic importance of lymph node metastases in dogs with appendicular osteosarcoma: 228 cases (1986-2003). J Am Vet Med Assoc 226, 1364-1367.

House, A.K., Catchpole, B., Gregory, S.P., 2007, Matrix metalloproteinase mRNA expression in canine anal furunculosis lesions. Vet Immun Immunopathol 115, 68-75.

Hong, S.H., Kadosawa, T., Mochizuki, M., Matsunaga, S., Nishimura, R., Sasaki, N., 1998, Establishment and characterization of two cell lines derived from canine spontaneous osteosarcoma. J Vet Med Sci 60, 757-760.

Isotani, M., Katsuma, K., Tamura, K., Yamada, M., Yagihara, H., Azakami, D., Ono, K., Washizu, T., Bonkobara, M., 2006, Efficient generation of canine bone marrow-derived dendritic cells. J Vet Med Sci 68, 809-814.

Jones, D.H., Nakashima, T., Sanchez, O.H., Kozieradzki, I., Komarova, S.V., Sarosi, I., Morony, S., Rubin, E., Sarao, R., Hojilla, C.V., Komnenovic, V., Kong, Y.Y., Schreiber, M., Dixon, S.J., Sims, S.M., Khokha, R., Wada, T., Penninger, J.M., 2006, Regulation of cancer cell migration and bone metastasis by RANKL. Nature 440, 692-696.

Kadosawa, T., Nozaki, K., Sasaki, N., Takeuchi, A., 1994, Establishment and characterization of a new cell line from a canine osteosarcoma. J Vet Med Sci 56, 1167-1169.

Khanna, C., Wan, X., Bose, S., Cassaday, R., Olomu, O., Mendoza, A., Yeung, C., Gorlick, R., Hewitt, S.M., Helman, L.J., 2004, The membrane-cytoskeleton linker ezrin is necessary for osteosarcoma metastasis. Nat Med 10, 182-186.

Kim, M.S., Lee, S.Y., Cho, W.H., Song, W.S., Koh, J.S., Lee, J.A., Yoo, J.Y., Jung, S.T., Jeon, D.G., 2008, Relationships between plain-film radiographic patterns and clinicopathologic variables in AJCC stage II osteosarcoma. Skeletal Radiol 37, 997-1001.

Kim, M.S., Song, W.S., Cho, W.H., Lee, S.Y., Jeon, D.G., 2007, Ezrin expression predicts survival in stage IIB osteosarcomas. Clin Ortho and related research 459, 229-236.

Kirpensteijn, J., Kik, M., Rutteman, G.R., Teske, E., 2002, Prognostic significance of a new histologic grading system for canine osteosarcoma. Vet Pathol 39, 240-246.

Knauper, V., Smith, B., Lopez-Otin, C., Murphy, G., 1997, Activation of progelatinase B (proMMP-9) by active collagenase-3 (MMP-13). Eur J Biochem 248, 369-373.

Knecht, C.D., Priester, W.A., 1978, Musculoskeletal tumors in dogs. 172, J Am Vet Med Assoc 72-74.

Kusano, K., Miyaura, C., Inada, M., Tamura, T., Ito, A., Nagase, H., Kamoi, K., Suda, T., 1998, Regulation of matrix metalloproteinases (MMP-2, -3, -9, and -13) by interleukin-1 and interleukin-6 in mouse calvaria:

association of MMP induction with bone resorption. Endocrinology 139, 1338-1345.

Lamoureux, F., Picarda, G., Rousseau, J., Gourden, C., Battaglia, S., Charrier, C., Pitard, B., Heymann, D., Redini, F., 2008, Therapeutic efficacy of soluble receptor activator of nuclear factor-kappa B-Fc delivered by nonviral gene transfer in a mouse model of osteolytic osteosarcoma. Mol Cancer Ther 7, 3389-3398.

Lamoureux, F., Richard, P., Wittrant, Y., Battaglia, S., Pilet, P., Trichet, V., Blanchard, F., Gouin, F., Pitard, B., Heymann, D., Redini, F., 2007, Therapeutic relevance of osteoprotegerin gene therapy in osteosarcoma: blockade of the vicious cycle between tumor cell proliferation and bone resorption. Cancer Res 67, 7308-7318.

Lana, S.E., Ogilvie, G.K., Hansen, R.A., Powers, B.E., Dernell, W.S., Withrow, S.J., 2000, Identification of matrix metalloproteinases in canine neoplastic tissue. Am J Vet Res 61, 111-114.

Lau, Y.S., Adamopoulos, I.E., Sabokbar, A., Giele, H., Gibbons, C.L., Athanasou, N.A., 2007, Cellular and humoral mechanisms of osteoclast formation in Ewing's sarcoma. Br J Cancer 96, 1716-1722.

Lee, J.A., Jung, J.S., Kim, D.H., Lim, J.S., Kim, M.S., Kong, C.B., Song, W.S., Cho, W.H., Jeon, D.G., Lee, S.Y., Koh, J.S., 2010, RANKL expression is related to treatment outcome of patients with localized, high-grade osteosarcoma. Ped Blood Cancer 56, 738-43

Ling, G.V., Morgan, J.P., Pool, R.R., 1974, Primary bone rumors in the dog: a combined clinical, radiographic, and histologic approach to early diagnosis. J Am Vet Med Assoc 165, 55-67.

Liptak, J.M., Dernell, W.S., Straw, R.C., Rizzo, S.A., Lafferty, M.H., Withrow, S.J., 2004, Proximal radial and distal humeral osteosarcoma in 12 dogs. J Am Anim Hosp Assoc 40, 461-467.

Loukopoulos, P., O'Brien, T., Ghoddusi, M., Mungall, B.A., Robinson, W.F., 2004, Characterisation of three novel canine osteosarcoma cell lines producing high levels of matrix metalloproteinases. Res Vet Sci 77, 131-141.

Loukopoulos, P., Robinson, W.F., 2007, Clinicopathological relevance of tumour grading in canine osteosarcoma. J Comp pathol 136, 65-73.

Lynch, C.C., Hikosaka, A., Acuff, H.B., Martin, M.D., Kawai, N., Singh, R.K., Vargo-Gogola, T.C., Begtrup, J.L., Peterson, T.E., Fingleton, B., Shirai, T., Matrisian, L.M., Futakuchi, M., 2005, MMP-7 promotes prostate cancer-induced osteolysis via the solubilization of RANKL. Cancer Cell 7, 485-496.

MacDougall, J.R., Matrisian, L.M., 1995, Contributions of tumor and stromal matrix metalloproteinases to tumor progression, invasion and metastasis. Cancer Metastasis Rev 14, 351-362.

McNeill, C.J., Overley, B., Shofer, F.S., Kent, M.S., Clifford, C.A., Samluk, M., Haney, S., Van Winkle, T.J., Sorenmo, K.U., 2007,

Characterization of the biological behaviour of appendicular osteosarcoma in Rottweilers and a comparison with other breeds: a review of 258 dogs. Vet Comp Oncol 5, 90-98.

Mee, A.P., May, C., Bennett, D., Sharpe, P.T., 1995, Generation of multinucleated osteoclast-like cells from canine bone marrow: effects of canine distemper virus. Bone 17, 47-55.

Misdorp, W., Hart, A.A., 1979, Some prognostic and epidemiologic factors in canine osteosarcoma. J Natl Cancer Inst 62, 537-545.

Miyamoto, N., Higuchi, Y., Mori, K., Ito, M., Tsurudome, M., Nishio, M., Yamada, H., Sudo, A., Kato, K., Uchida, A., Ito, Y., 2002, Human osteosarcoma-derived cell lines produce soluble factor(s) that induces differentiation of blood monocytes to osteoclast-like cells. Intern Immunopharmacol 2, 25-38.

Miyazaki, T., Katagiri, H., Kanegae, Y., Takayanagi, H., Sawada, Y., Yamamoto, A., Pando, M.P., Asano, T., Verma, I.M., Oda, H., Nakamura, K., Tanaka, S., 2000, Reciprocal role of ERK and NF-kappaB pathways in survival and activation of osteoclasts. J Cell Biol 148, 333-342.

Mori, K., Ando, K., Heymann, D., Redini, F., 2009, Receptor activator of nuclear factor-kappa B ligand (RANKL) stimulates bone-associated tumors through functional RANK expressed on bone-associated cancer cells? Histol Histopathol 24, 235-242.

Mori, K., Le Goff, B., Berreur, M., Riet, A., Moreau, A., Blanchard, F., Chevalier, C., Guisle-Marsollier, I., Leger, J., Guicheux, J., Masson, M., Gouin, F., Redini, F., Heymann, D., 2007, Human osteosarcoma cells express functional receptor activator of nuclear factor-kappa B. J Pathol 211, 555-562.

Mundy, G.R., 2002, Metastasis to bone: causes, consequences and therapeutic opportunities. Nat Rev Cancer 2, 584-593.

Nannuru, K.C., Futakuchi, M., Sadanandam, A., Wilson, T.J., Varney, M.L., Myers, K.J., Li, X., Marcusson, E.G., Singh, R.K., 2009, Enhanced expression and shedding of receptor activator of NF-kappaB ligand during tumor-bone interaction potentiates mammary tumor-induced osteolysis. Clin Exp Metastasis 26, 797-808.

Nelson, J.B., Hedican, S.P., George, D.J., Reddi, A.H., Piantadosi, S., Eisenberger, M.A., Simons, J.W., 1995, Identification of endothelin-1 in the pathophysiology of metastatic adenocarcinoma of the prostate. Nat Med 1, 944-949.

Norrdin, R.W., Powers, B.E., Torgersen, J.L., Smith, R.E., Withrow, S.J., 1989, Characterization of osteosarcoma cells from two sibling large-breed dogs. Am J Vet Res 50, 1971-1975.

Nagase, Y., Iwasawa, M., Akiyama, T., Kadono, Y., Nakamura, M., Oshima, Y., Yasui, T., Matsumoto, T., Hirose, J., Nakamura, H., Miyamoto, T., Bouillet, P., Nakamura, K., Tanaka, S., 2009, Anti-apoptotic molecule Bcl-2 regulates the differentiation, activation, and survival of both

osteoblasts and osteoclasts. J Biol Chem 284, 36659-36669.

Patnaik, A.K., 1990, Canine extraskeletal osteosarcoma and chondrosarcoma: a clinicopathologic study of 14 cases. Vet Pathol 27, 46-55.

Roodman, G.D., 2004, Mechanisms of bone metastasis. N Engl J Med 350, 1655-1664.

Ru, G., Terracini, B., Glickman, L.T., 1998, Host related risk factors for canine osteosarcoma. Vet J 156, 31-39.

Sago, K., Tamahara, S., Tomihari, M., Matsuki, N., Asahara, Y., Takei, A., Bonkobara, M., Washizu, T., Ono, K., 2008, In vitro differentiation of canine celiac adipose tissue-derived stromal cells into neuronal cells. J Vet Med Sci 70, 353-357.

Selvarajah, G.T., Kirpensteijn, J., van Wolferen, M.E., Rao, N.A., Fieten, H., Mol, J.A., 2009, Gene expression profiling of canine osteosarcoma reveals genes associated with short and long survival times. Mol Cancer 8, 72.

Snoek-van Beurden, P.A., Von den Hoff, J.W., 2005, Zymographic techniques for the analysis of matrix metalloproteinases and their inhibitors. Biotechniques 38, 73-83.

Spahni, A.I., Schawalder, P., Rothen, B., Bosshardt, D.D., Lang, N., Stoffel, M.H., 2009, Immunohistochemical localization of RANK, RANKL and

OPG in healthy and arthritic canine elbow joints. Vet Surg 38, 780-786.

Spodnick, G.J., Berg, J., Rand, W.M., Schelling, S.H., Couto, G., Harvey, H.J., Henderson, R.A., MacEwen, G., Mauldin, N., McCaw, D.L., et al., 1992, Prognosis for dogs with appendicular osteosarcoma treated by amputation alone: 162 cases (1978-1988). J Am Vet Med Assoc 200, 995-999.

Straw, R.C., Withrow, S.J., Powers, B.E., 1990, Management of canine appendicular osteosarcoma. Vet Clin North Am Small Anim Pract 20, 1141-1161.

Suda, T., Takahashi, N., Martin, T.J., 1992, Modulation of osteoclast differentiation. Endoc Rev 13, 66-80.

Suda, T., Takahashi, N., Udagawa, N., Jimi, E., Gillespie, M.T., Martin, T.J., 1999, Modulation of osteoclast differentiation and function by the new members of the tumor necrosis factor receptor and ligand families. Endoc Rev 20, 345-357.

Sugiura, Y., Shimada, H., Seeger, R.C., Laug, W.E., DeClerck, Y.A., 1998, Matrix metalloproteinases-2 and -9 are expressed in human neuroblastoma: contribution of stromal cells to their production and correlation with metastasis. Cancer Res 58, 2209-2216.

Wagner, E.F., 2002, Functions of AP1 (Fos/Jun) in bone development. Ann Rheum Dis 61 Suppl 2, ii40-42.

Withrow, S.J., Vail, D.M. 2007. Small Animal Clinical Oncology. In Tumors of the skeletal system, Dernell, W.S., Ehrhart, N.P., Straw, R.C., Vail, D.M.,eds. (St. Louis, SAUNDERS), pp.540-582

Wittrant, Y., Theoleyre, S., Chipoy, C., Padrines, M., Blanchard, F., Heymann, D., Redini, F., 2004, RANKL/RANK/OPG: new therapeutic targets in bone tumours and associated osteolysis. Biochim Biophys Acta 1704, 49-57.

Yue, W., Sun, Q., Landreneau, R., Wu, C., Siegfried, J.M., Yu, J., Zhang, L., 2009, Fibulin-5 suppresses lung cancer invasion by inhibiting matrix metalloproteinase-7 expression. Cancer Res 69, 6339-6346.